Journal of Visualized Experiments

Crystallization of proteins on chip by microdialysis for in situ X-ray diffraction studies

--Manuscript Draft--

Article Type:	Invited Methods Article - Author Produced Video
Manuscript Number:	JoVE61660R2
Full Title:	Crystallization of proteins on chip by microdialysis for in situ X-ray diffraction studies
Corresponding Author:	Monika Budayova - Spano Institut de Biologie Structurale Grenoble, France FRANCE
Corresponding Author's Institution:	Institut de Biologie Structurale
Corresponding Author E-Mail:	monika.spano@ibs.fr
Order of Authors:	Sofia Jaho
	Niels Junius
	Franck Borel
	Yoann Sallaz-Damaz
	Jean-Baptiste Salmon
	Monika Budayova-Spano
Additional Information:	
Question	**Response**
Please indicate whether this article will be Standard Access or Open Access.	Standard Access (US$1200)
Please confirm that you have read and agree to the terms and conditions of the author license agreement that applies below:	I agree to the Author License Agreement
Please specify the section of the submitted manuscript.	Chemistry
Please provide any comments to the journal here.	We addressed all comments raised by editorial team and referees and hope that the revised version of the manuscript as well as the video will be suitable for publication.

TITLE:

Crystallization of Proteins on Chip by Microdialysis for In Situ X-ray Diffraction Studies

AUTHORS AND AFFILIATIONS:

Sofia Jaho[1], Niels Junius[1]*, Franck Borel[1], Yoann Sallaz-Damaz[1], Jean-Baptiste Salmon[2], Monika Budayova-Spano[1]

[1]Université Grenoble Alpes, CEA, CNRS, IBS, Grenoble, France
[2]CNRS, Solvay LOF, UMR 5258, Université Bordeaux, Pessac, France

*Current address: Elvesys, Paris, France

Email addresses of co-authors:

Sofia Jaho	(sofia.jaho@ibs.fr)
Niels Junius	(niels.junius@elvesys.com)
Franck Borel	(franck.borel@ibs.fr)
Yoann Sallaz-Damaz	(yoann.sallaz-damaz@ibs.fr)
Jean-Baptiste Salmon	(jean-baptiste.salmon-exterieur@solvay.com)
Monika Budayova-Spano	(monika.spano@ibs.fr)

Corresponding author:

Monika Budayova-Spano (monika.spano@ibs.fr)

KEYWORDS:

microfluidics, on-chip protein crystallization, in situ X-ray diffraction, microdialysis crystallization, serial crystallography, phase diagrams, dialysis chip

SUMMARY:

This paper details the fabrication protocol of microfluidic chips developed for on-chip protein crystallization with the dialysis method and in situ X-ray diffraction experiments. The microfabrication process makes it possible to integrate a semipermeable regenerated cellulose dialysis membrane with any molecular weight cut-off, between two layers of the chip.

ABSTRACT:

This protocol describes the manufacturing of reproducible and inexpensive microfluidic devices covering the whole pipeline for crystallizing proteins on-chip with the dialysis method and allowing in situ single-crystal or serial crystallography experiments at room temperature. The protocol details the fabrication process of the microchips, the manipulation of the on-chip crystallization experiments and the treatment of the in situ collected X-ray diffraction data for the structural elucidation of the protein sample. The main feature of this microfabrication procedure lies on the integration of a commercially available, semipermeable regenerated cellulose dialysis membrane in between two layers of the chip. The molecular weight cut-off of the embedded membrane varies depending on the molecular weight of the macromolecule and the precipitants. The device exploits the advantages of microfluidic technology, such as the use

of minute volumes of samples (<1 µL) and fine tuning over transport phenomena. The chip coupled them with the dialysis method, providing precise and reversible control over the crystallization process and can be used for investigating phase diagrams of proteins at the microliter scale. The device is patterned using a photocurable thiolene-based resin with soft imprint lithography on an optically transparent polymeric substrate. Moreover, the background scattering of the materials composing the microchips and generating background noise was evaluated rendering the chip compatible for in situ X-ray diffraction experiments. Once protein crystals are grown on-chip up to an adequate size and population uniformity, the microchips can be directly mounted in front of the X-ray beam with the aid of a 3D printed holder. This approach addresses the challenges rising from the use of cryoprotectants and manual harvesting in conventional protein crystallography experiments through an easy and inexpensive manner. Complete X-ray diffraction data sets from multiple, isomorphous lysozyme crystals grown on-chip were collected at room temperature for structure determination.

INTRODUCTION:

Elucidating the three-dimensional (3D) structure of biological macromolecules is an unceasing pursuit in structural biology where X-ray crystallography remains the principal investigation technique. Applied for unraveling the structural details of complex macromolecules, such as proteins, it aims at facilitating the understanding of their mechanisms of actions and their involvement in various biological functions. Powerful X-ray sources at synchrotrons and X-ray free-electron lasers (XFELs) provide all the tools required for a deeper insight into the proteins' structure at near atomic resolution. Despite the advantages that come along with the use of X-rays for structural studies, there are limitations intrinsic to X-ray radiation and the crystallization process itself. Radiation damage provoked by high X-ray flux and long exposure times of the protein crystal in front of the X-ray beam are restrictive parameters that crystallographers have to surpass using cryogenic cooling[1]. However, finding the optimal cryocooling conditions can be laborious since conformational changes from the native protein structure or artifacts can be concealed[2,3]. Moreover, recent studies indicate that performing diffraction experiments at room temperature leads to lower specific radiation damage[4]. Another bottleneck in structural biology is the acquisition of well-diffracting crystals with a sufficient size[5]. Small crystals are easier to produce, especially in the case of membrane proteins, but are more susceptible to radiation damage even under cryocooling conditions because a high radiation dose must be directed in a smaller volume compared to the case of larger protein crystals[6]. The novel approach of serial crystallography[7,8] at synchrotrons and XFELs can circumvent the restrains of radiation damage and at the same time exploit smaller crystals (200 nm to 2 µm)[7] by merging data sets from multiple, isomorphous and randomly oriented protein crystals and profiting from the associated technological advances such as femtosecond pulses, shorter exposure times and micro-focused X-ray beams[5,7,9,10].

Microfluidic technology is valuable to X-ray crystallography, exhibiting manifold advantages for the crystallization of biological macromolecules and their structural investigation. Conducting crystallization experiments in microfluidic devices requires small volumes of protein sample, therefore constraining the production cost of these high-valued bio macromolecules and facilitating high-throughput screening and optimization of numerous crystallization conditions.

Moreover, the inherent large surface area-to-volume ratio at the microfluidic scale and diffusion-limited transport phenomena enable fine control over flows and temperature or concentration gradients[11–14], rendering microfluidic devices suitable for growing uniformly sized crystals and exploring phase diagrams[15–19]. Moreover, microfluidic tools display a distinctive potential to address another hurdle in protein crystallography, which is the sample delivery, and the necessity to handle and harvest protein crystals prior to their use for X-ray diffraction experiments. The method of on-chip and in situ X-ray crystallography eliminates the crystal manipulation and the potential deterioration of crystal quality prior to data collection. A wide range of microfluidic chips compatible for in situ X-ray protein crystallography have been designed, developed, and tested by many research groups confronting the related restrictions arising from the nature of the microfabrication materials and their interactions with X-rays[14,19,20–23]. The fabrication materials must be optically transparent, biologically inert and demonstrate high transparency to X-ray radiation and an optimal signal-to-noise ratio during data collection.

Most of the crystallization methods applied in conventional protein crystallography[24,25] have also been implemented at the microfluidic scale[11,14] for on chip crystallization and in situ X-ray diffraction analysis. Simple, hybrid, or multi-layered microfluidic apparatus incorporating vapor diffusion[26], evaporation[27], free interface diffusion (FID)[28], microbatch[26], or even seeding[29] have been used to crystallize soluble and membrane proteins. High throughput screening and optimization of crystallization conditions can be achieved[30,31] in well-based[32], droplet-based[33], or valve-actuated[34] devices. In situ X-ray diffraction experiments of challenging protein targets at room temperature have been conducted in microchips fabricated from various materials such as PDMS (polydimethylsiloxane), COC (cyclic olefin copolymer), PMMA (poly(methyl methacrylate))[21,22,26,28,29], graphene films[23], Kapton[35], epoxy glue[6], or NOA (Norland optical adhesive)[19] and the materials' transparency to X-ray radiation and their contribution to background noise have been evaluated. Moreover, microchips have been designed to couple the in situ and the serial data collection strategies in a single tool for X-ray protein crystallography experiments at synchrotron sources[23,35,36] and XFELs[7].

Room temperature, in situ data collection has also been implemented in various delivery methods and devices. For example, Nogly et al.[54] used a lipidic cubic phase (LCP) injector in order to study the structure of the light-driven photon pump bacteriorhodopsin (bR) by serial femtosecond crystallography (SFX) using an XFEL source. The crystal structure of bR was solved to 2.3 Å resolution, demonstrating the compatibility of an LCP injector with time-resolved serial femtosecond crystallography (TR-SFX). Baxter et al.[55] designed a high-density multi-crystal grid, fabricated by a 100 or 200 μm thick polycarbonate plastic with laser-cut holes of various sizes. An additional 5 μm thick polycarbonate film can be fixed to one side of the grid when using the device for sitting- or hanging-drop crystallization experiments. This high-density grid can be used in multiple ways as crystals can be loaded directly onto the ports of the device or crystals can be grown on the device by vapor diffusion or the LCP method. Moreover, the grid can be adjusted in a standard magnetic base and used for in situ X-ray data collection at cryogenic or room temperature conditions. More recently, Feiler et al.[56] developed a sample holder for macromolecular in situ X-ray crystallography at cryogenic and ambient temperature with

minimal background noise contribution. Specifically, the holder comprises a plastic support, a transparent COC foil and a microporous structured polyimide foil. It was designed to replace the commonly used cover slides for setting up crystallization drops, while allowing in-place manipulation such as ligand soaking, complex formation, and cryogenic protection without opening the crystallization drop or manually handling the crystals. Moreover, the sample holder can be removed from the crystallization plate and placed onto a magnetic base for in situ data collection at standard goniometer-based beamlines. For ambient temperature data collection, the COC foil is removed prior to the experiment and only the 21 µm-thick polyimide foil contributes to background scattering, which in this case is minimal. These examples compose only a small fraction of the ongoing research and the multitude of versatile microchips developed for X-ray protein crystallography.

However, the dialysis protein crystallization method has not been widely incorporated within microfluidics. Dialysis is a diffusion-based method aiming for the equilibration of precipitant concentration through a semi-permeable membrane in order to approach the nominal concentration for protein crystallization and enables precise and reversible control over the crystallization conditions[24]. The Molecular Weight Cut-Off (MWCO) of the semi-permeable dialysis membrane can be chosen depending on the molecular weight of the macromolecule and the precipitants to allow the diffusion of small precipitant molecules while retaining the macromolecule of interest. Due to the reversibility of the dialysis process, it can be used in combination with temperature control to decouple and optimize nucleation and crystal growth independently[37] for investigating phase diagrams by altering the precipitant concentration while using the same protein sample. The integration of membranes in microfluidics is reviewed by de Jong et al.[38] and the case studies in biology implanting dialysis into microchips can be principally listed in sample preparation, concentration or filtration applications[39–42] or cell-related studies[43,44]. Pervaporation through PDMS was used by Shim et al.[37] to study the nucleation and growth of xylanase in various conditions. Water permeated through the 15 µm thick PDMS membrane into the protein reservoir of the microfluidic device, subsequently altering the protein and precipitant concentration.

The protocol developed by Junius et al.[19,45] for the fabrication of a microfluidic chip compatible for both on-chip protein crystallization via microdialysis and in situ X-ray diffraction experiments at room temperature is presented. The protocol for the device fabrication is directly inspired by the pioneering work accomplished by Studer and coworkers[12,46] for micro-patterned stickers of photo-curable thiolene-based resin NOA 81 embedding commercially available membranes, using soft imprint lithography. An innovative modification of the method resulted in microchips enabling the use of microdialysis to accurately monitor and control the experimental parameters for the on-chip growth of protein crystals and simultaneously exploits the advantages of microfluidics, such as reduced consumption of protein samples per experiment (<1 µL). In a previous work, the principles of dialysis applied to a macro-scale system (typical volume >20 µL) for screening and optimizing crystallization conditions by mapping temperature-precipitant concentration phase diagrams were demonstrated[47]. In this work, a protocol is described for producing dialysis microchips incorporating regenerated cellulose (RC) dialysis membranes of different MWCO in order to perform crystallization assays

on-chip and in situ X-ray diffraction data collection. The materials comprising the microchips have been evaluated for their transparency to X-rays[19] and the devices can be set directly in front of the X-ray beam for room temperature in situ diffraction experiments, excluding the manual handling and minimizing the degradation of fragile protein crystals. In a case study, hen white-egg lysozyme crystals were grown on-chip via microdialysis generating a uniformly sized population. The microchip was then mounted in front of the X-ray beam with a 3D-printed support[19] and complete in situ diffraction data sets were collected at room temperature from multiple, isomorphous crystals, demonstrating the high potential and relevance of the chips for synchrotron serial crystallography studies of challenging macromolecular targets.

PROTOCOL:

1. Mask design and master fabrication

1.1. Draw the desired geometries of the microfluidic device using any vectorial drawing software. For each layer of the photoresist that will be used for the next step of photolithography, prepare an individual mask: one mask outlined with channels and pillars and one mask containing only the pillars.

1.2. Translate the CIF files generated by the drawing software into film photomasks. This can be done through commercial services. Require the appropriate photomask depending on the choice of photoresist used during photolithography.

NOTE: For the SU-8 photoresist, order masks with black features on a transparent background. SU-8 is an epoxy-based negative photoresist, which means that during the exposure to UV light (365 nm) the parts exposed to UV are crosslinked whereas the rest remains soluble. SU-8 is a negative photoresist and all black patterns on the mask will not be cross-linked by UV light during the photolithography. Hence, channels and pillars will be engraved on the masters.

1.3. Prepare two masters on silicon wafers for each chip's design by photolithography using SU-8 negative photoresist.

NOTE: Steps 1.3.1–1.3.7 are performed in a clean room. The steps described below are the traditional steps of photolithography followed by PDMS soft lithography, which are described in many textbooks. All the values of the experimental parameters (photoresist, time duration, temperature, etc.) depend on many subtle parameters and have to be optimized depending on the different apparatus used.

1.3.1. Use a 3-inch silicon wafer and treat the surface with plasma for 90 s, in order to facilitate the deposition and attachment of the SU-8 photoresist.

1.3.2. Pour roughly 1 mL of SU-8 resist on the middle of the wafer and spin coat the SU-8 down to the desired thickness (**Figure 1A**). For 50 µm nominal thickness, use SU-8 3050 and spin coat for 10 s at 500 rpm and successively for 30 s at 3,500 rpm. Soft bake the photoresist

on a hot plate for 15 min at 368 K in order to be partially solidified by allowing the solvent contained in the resin to evaporate and prevent it from sticking on the photomask. Afterwards, leave the wafer at room temperature for 2 min.

1.3.3. Expose the photoresist to UV light (**Figure 1B**). Use a mask aligner with a power of 35 mW cm^{-2} and 8 s exposure time.

1.3.4. Proceed with the post-exposure baking. Place the wafer on a hot plate for 5 min at 368 K to complete the photoreaction invoked by the UV exposure.

1.3.5. Remove all the SU-8 resist that was not crosslinked by placing the wafer in a bath containing propylene glycol methyl ether acetate (PGMEA) and stir for 15 min. Rinse the wafer with isopropanol until no blurry precipitation can be observed. Dry the wafer with nitrogen gas and store it in a Petri dish (100 mm x 15 mm standard size).

1.3.6. Treat the surface of the wafer with a silane in order to facilitate the detachment of polydimethylsiloxane (PDMS) that will be used to fabricate 2 stamps. Deposit the wafer on a tapped hot plate at 368 K for 10 min under the vapor atmosphere of hexamethyldisilazane (HMDS).

NOTE: If peeling off the PDMS from the wafer becomes difficult after several uses, the surface of the wafer should be treated again with HMDS vapor.

1.3.7. The first master containing the channels and the pillars is ready. Repeat these steps and prepare the second master patterning only the pillars.

NOTE: During photolithography, the aim is to obtain the geometries of the device on the SU-8 masters with a height of 50 µm. However, once the two SU-8 masters are fabricated, measure the height of the geometries engraved on the masters with a profilometer in order to acquire the experimental value. The measured value for both SU-8 masters fabricated for this protocol is approximately 45 µm.

2. PDMS molds fabrication

NOTE: The following steps of the protocol can be performed in any laboratory as long as a laminar flow hood is used, yellow light in the room is used when working with the NOA 81 resin (steps 3.6–3.11) and a source of UV light is available for polymerizing the NOA 81 resin (steps 3.7 and 3.11).

2.1. Prepare 50 g of PDMS silicone base and its curing agent in a 10:1 mass ratio.

2.2. Mix both the ingredients in a beaker with a spatula and place the mixture in a vacuum chamber to remove all the air bubbles.

2.3. Pour 25 g of the pre-mixed PDMS into the SU-8 master (stored in a Petri dish) patterning the channels and the pillars up to a height of approximately 5 mm. Pour the remaining 25 g of the PDMS into the second SU-8 master patterning only the pillars up to a height of approximately 5 mm (**Figure 1C**).

2.4. Place both the Petri dishes in an oven and cure the PDMS layers at 338 K for 1 h.

2.5. Cut the cured PDMS layer around the patterns of the SU-8 masters with a scalpel and gently peel off the PDMS molds from the masters (**Figure 1D**).

NOTE: The procedure described above, called replica molding, is frequently being used to prepare molds of PDMS that will be attached to glass surfaces and be part of a microfluidic device[53]. In this protocol, the PDMS molds are not part of the chip, but they are used as intermediates for the chip fabrication. For each design, 2 PDMS molds are prepared from the respective SU-8 masters (**Figure 1D and E**) and will be used accordingly (as described below) for the fabrication of the microchip.

3. Dialysis chip fabrication

3.1. Place the PDMS mold patterning both the channels and pillars on a rigid microscope glass slide (3 x 1 in. standard size) with the patterns facing upwards (**Figure 1F**). The central pillar that corresponds to the protein reservoir exceeds vertically by 45 µm from the horizontal surface of the PDMS mold.

3.2. Cut and separate a dry piece of the regenerated cellulose (RC) dialysis membrane and deposit it on the central pillar of the PDMS mold, which is supported on the glass slide (**Figure 1F**).

NOTE: The RC dialysis membrane is commercially available, and the molecular weight cut-off (MWCO) is chosen accordingly with the molecular weight of the protein under study and the precipitants used. The size of the piece of the RC dialysis membrane depends on the design of the chip. In this protocol, 2 prototypes are designed where the volume of the protein reservoir is 0.1 or 0.3 µL. In these cases, the size of the dialysis membrane piece is 2 x 2 mm^2 or 4 x 4 mm^2, respectively.

3.3. Place the second PDMS mold patterning only the pillars facing downwards on top of the PDMS mold supported on the glass slide (**Figure 1F**). The central pillar of this mold corresponds to the protein reservoir and exceeds vertically (facing downwards) by 45 µm from the horizontal surface.

3.4. Align the central pillars of the 2 PDMS molds. The RC dialysis membrane is “sandwiched” in between the 2 PDMS molds (**Figure 1G**).

NOTE: The alignment between the microstructures of the 2 PDMS molds can be accomplished

visually, without any extra equipment. Otherwise, this manipulation can be achieved under a microscope. A small shift between the reservoirs is not problematic, as long as the fluidic channel and the input or output points are not entirely covered.

3.5. Desiccate the assembly for 30 min in a vacuum chamber to remove all trapped air bubbles in the PDMS molds and to promote the insertion of the resin during the next step of the fabrication.

NOTE: The 2 PDMS molds are kept in place by PDMS-PDMS adhesion and no extra pressure or other way of temporary bonding is required.

3.6. Fill the empty space between the 2 PDMS molds with the photocurable, thiolene-based resin NOA 81 by capillary imbibition (**Figure 1H,I**).

3.7. Cure the resin by exposure to UV light (365 nm) for 8 s using a collimated UV lamp (power 35 mW cm^{-2}).

NOTE: This first exposure allows NOA 81 resin to be partially crosslinked since a thin layer of NOA 81 in contact with the PDMS molds on both sides remains uncured.

3.8. Cut the excess of NOA 81 from the external sides of the PDMS molds with a scalpel.

3.9. Remove the upper PDMS mold with the partially crosslinked NOA 81 stuck on it from the bottom PDMS mold and the glass slide.

3.10. Cut a 175 µm thick PMMA sheet in the standard dimensions of a microscope glass slide (3 x 1 inches) and peel off the plastic protection sheets from each side of the PMMA piece. Gently press the assembly of the upper PDMS mold and the partially cured NOA 81 on the PMMA piece (**Figure 1J**).

3.11. Cure again NOA 81 by exposure to UV light for 60 s and remove the upper PDMS mold (**Figure 1K**). The resin adheres to the PMMA substrate without any further treatment.

NOTE: The PDMS molds can be reused approximately up to 5 times after washing them with isopropanol and acetone, as long as the molds are not bent. The RC dialysis membrane is incorporated into the NOA 81 sticker and no further manipulation or mechanical clamping is required.

4. Fluidic connectors

NOTE: The design of the microfluidic chip consists of a linear fluidic channel for the crystallization solution and a central reservoir for the protein sample (protein reservoir), both shown from a top view of two microchips in **Figure 1A**. A RC dialysis membrane is embedded between these two microstructures (**Figure 2D**) and the crystallization process evolves while

precipitants from the crystallization solution diffuse across the membrane due to a concentration gradient between the two compartments of the chip that are separated by the membrane. The microfluidic channel is imprinted on the bottom PDMS mold (**Figure 1F**). Once the fabrication protocol for the chips is completed, the linear channel is located on the bottom layer of the NOA 81 sticker in contact with the PMMA substrate, as shown in **Figure 1K**. An inlet and an outlet access point for the crystallization solution are located at each end of the linear channel and look like holes (total height 90 µm) as can be seen in **Figure 2A**. For the handling of the crystallization solution, connectors must be added on the access points.

4.1. Bond connectors are commercially available (NanoPort) on the inlet and outlet of the microfluidic channel with fast epoxy glue (**Figure 2C**).

4.2. Choose the appropriate diameter of the PTFE tubes based on the size of the connectors. The PTFE tubes will be used for the introduction of the crystallization solution in the fluidic channel of the chip.

NOTE: Commercially available kits are recommended for easy and precise control over the flow rate and are usually combined with automated pressure-driven or flow controlled (syringe pumps) systems for mixing and fluid handling. However, the crystallization solution can be introduced manually into the linear channel with a disposable plastic syringe. In this case, steps 4.3 to 4.5 are suggested.

4.3. Fill a 1 mL disposable syringe with the crystallization solution. For the chips presented in this protocol, 400 µL is sufficient in order to fill up the whole fluidic channel.

4.4. Cut two pipette tips so that the diameter of the tip at one side is equal to the inner diameter of the PTFE tube that will be used for the solution handling. Glue the cropped tips on the access points of the channel with fast epoxy glue (**Figure 2B**).

4.5. Connect the syringe with the cropped tips with a piece of PTFE tube of the appropriate size and introduce the solution within the channel by constantly pushing the syringe plunger slowly.

5. Protein encapsulation

NOTE: The pattern of the chip dedicated to being used as the protein reservoir remains so far open to the atmosphere. The following protocol is proposed to carefully confine the protein sample within the microfluidic chip.

5.1. Manually pipette a droplet of the protein sample inside the protein reservoir, located right upon the RC dialysis membrane, as illustrated in **Figure 2E**. The volume of the protein sample varies according to the design of the chip and can be 0.1 or 0.3 µL.

5.2. Apply a thin layer of high-vacuum silicone grease all around the protein reservoir.

5.3. Cut a small piece of a 175 µm thick PMMA sheet and gently place it above the thin layer of the silicone grease. The PMMA piece must cover the whole surface of the protein reservoir where the protein solution is deposited.

NOTE: The silicone grease is used to enhance air-tightness and prevent the spreading of the protein droplet. There is no bonding or sealing between the PMMA piece used for covering the protein reservoir and the NOA 81 sticker. The contact between them is a solid/solid interface. In order to produce an overall sealing and an air-tight encapsulation of the protein sample, a piece of Kapton tape is used as described in step 5.4.

NOTE: It is sometimes difficult to confine the protein sample within the dedicated cavity of the device (protein reservoir) when a pressure-driven system is used for the introduction of the crystallization solution within the fluidic channel (step 6.4). To avoid the problem mentioned above, relatively low pressure values should be maintained while circulating the crystallization solution. An injection pressure of 20–60 mbar for aqueous solutions or 50–150 mbar for more viscous solutions (PEGs, glycerol) is suggested[19].

5.4. Cut a piece of Kapton tape (20 µm thick) large enough to cover the PMMA piece set above the protein reservoir and to stick on the NOA chip around all edges. The protein sample is encapsulated within the reservoir and the chip is ready to be used for the crystallization experiment, as shown in **Figure 2C**.

NOTE: The chips can be reused several times as long as the dialysis membrane and the adhesion of NOA on the PMMA substrate are not deteriorated. If these parts of the chip are damaged, leaks are observed verifying that the device can no longer be used. Washing the chips depends on the crystallization solution. In the case of low viscosity solutions (salts, buffers), the fluidic channel can be washed by merely introducing distilled water and let it flow for a few minutes. 400 µL is the volume required in order to completely exchange a solution within the channel with another solution. In the case of more viscous solutions (PEGs, glycerol), reusing the chips is not recommended since washing the channel only with water is not sufficient. The upper part of the chip, where the protein reservoir is located, can also be washed with distilled water and dried with pressurized air.

6. On-chip protein crystallization

6.1. Weigh lyophilized hen egg-white lysozyme powder and dissolve in distilled water to obtain a final concentration of 30 mg mL^{-1}.

6.2. Filter the protein solution through a 0.22 µm filter and centrifuge for 5 min at the highest speed at 293 K to remove all solid particles. Use the supernatant for the crystallization experiment.

6.3. Prepare 500 µL of crystallization solution containing the buffer and the precipitant in

concentrations provided in **Table 1**. Filter the solution through a 0.22 µm filter.

6.4. Inject the solution into the inlet point of the chip with a syringe or an automated pressure-driven fluidic system or a syringe pump, as described in steps 4.1–4.5.

NOTE: The crystallization experiment can occur either under static condition, if the microfluidic channel is filled with the crystallization solution and set aside, or under flowing conditions, if it is continuously injected inside the channel at a constant flow rate. For the latter case, the use of an external pressure-driven system or syringe pump is recommended. The realization of the experiment under flowing conditions also provides the possibility to dynamically exchange crystallization solutions within the fluidic channel. Thus, multiple experiments can be conducted while using the same protein sample.

6.5. Once the fluidic channel is filled with the crystallization solution, seal the inlet and outlet ports of the chip with parafilm tape.

6.6. Pipette the appropriate volume of the protein solution within the protein reservoir and encapsulate the protein sample as described in steps 5.1–5.4.

6.7. Store the chip at 293 K.

NOTE: Crystallization via dialysis follows a different kinetic trajectory from experiments conducted with the vapor diffusion method or batch crystallization and depends profoundly on the nature of precipitant molecules involved in the diffusion process, according to measured data[51], and it might take more time for the nucleation to start. In order to prevent evaporation, if any, during this period, place the chip in a humidity saturated atmosphere at 293 K.

7. In situ and on-chip X-ray diffraction

7.1. 3D printed support for beamlines

7.1.1. Print the support that can carry up to three chips simultaneously. The dimensions of the support are the same as the dimensions of commercial crystallization plates (96 well/SBS standard) compatible with in plate X-ray diffraction experiments.

NOTE: The printing of the support can be assigned to commercial services. The support was designed using a 3D-CAD designing software and is shown in **Figure 3A** during on-chip protein crystallization experiments and in **Figure 3B** during in situ X-ray diffraction data collection at BM30A-FIP (ESRF).

7.1.2. Stabilize the dialysis chips on the support with a single- or double-sided tape.

7.2. In situ X-ray diffraction

7.2.1. Collect X-ray diffraction data at room temperature from crystals grown in the protein reservoir. For instance, use X-rays with an energy of 12.656 keV, a flux of 3.32 x 10^{10} photons s^{-1} and a beam size of 250 x 250 μm^2. Record the diffraction images with an ADSC Quantum 315r detector with a matrix of 3 x 3 CCD for an active surface of 315 x 315 mm^2 and 9.4 mega pixels resolution.

NOTE: The diffraction data for the lysozyme crystals grown on the dialysis chips were collected at BM30A-FIP beamline at the European Synchrotron Radiation Facility (ESRF). However, the beam size, the flux and the detector type may be different in other X-ray radiation sources. The 3D printed support enables data collection with an angular range of -40° to +40° around the crystal. The number of the lysozyme crystals exposed for in situ data collection, the number of the diffraction patterns collected for each crystal, the oscillation angle range per exposure and the exposure time are summarized in **Table 2**.

7.3. Data treatment

7.3.1. Process the complete or partial data sets with the diffraction patterns for the lysozyme crystals with the XDS program[48].

7.3.2. Generate the HKL file for each data set and scale them using the XSCALE software[48].

7.3.3. Use molecular replacement with the program Phaser of the CPP4 suite[49] and determine the phases for model building. For this step, use the known 3D coordinates of lysozyme from the Protein Data Bank (PDB) entry 193L.

7.3.4. Refine the structure using Phenix[52] and inspect the final protein model using COOT[50].

REPRESENTATIVE RESULTS:

The microfluidic chips developed by Junius et al.[19,45] are compatible for both on-chip protein crystallization with the microdialysis method and in situ X-ray diffraction data collection at room temperature. Pictures of the microchips, their detailed design, the fluidic connectors, and the RC dialysis membrane are illustrated in **Figure 2**. The crystallization experiments are set up by manually pipetting the protein sample directly into the protein reservoir and introducing the crystallization solution into the linear fluidic channel with an automated pressure-driven system or syringe pump or manually with the aid of a syringe. The protein reservoir and the fluidic channel can be distinguished in **Figure 2A**. Designs for fabricating chips with 0.1 µL or 0.3 µL maximum volume of the protein reservoir are shown in **Figure 2A** on the left and right, respectively. Chips with a 0.2 µL or 0.7 µL maximum capacity for the protein sample are shown elsewhere[19]. The highlight of the protocol for the device fabrication can be narrowed down on the use of the photocurable thiolene-based resin NOA 81 embedding commercially available RC dialysis membranes of various MWCOs. During the fabrication of the microfluidic devices, the linear fluidic channel is imprinted on the bottom PDMS mold (**Figure 1F**), while the upper PDMS mold consists only of the patterned pillars for the protein reservoir and the inlet and outlet ports (**Figure 1F**). Once NOA 81 is crosslinked and the PDMS molds are removed from the

assembly (**Figure 1K**), the fluidic channel is located at the bottom layer of the microchip and the protein channel and inlet/outlet ports are located on both layers. **Figure 1L** illustrates a side view schematic of the dialysis chip where all the layers of the device and their respective thickness are indicated. The height of the patterns imprinted on the bottom layer of the chips (fluidic channel) is approximately 45 µm, while the total height of the inlet and outlet ports is approximately 90 µm. The protein reservoir (45 µm height) is also illustrated in **Figure 2D,E**. The alignment of the two layers was investigated under an optical microscope and the piece of the RC dialysis membrane incorporated within the microchip can be clearly distinguished in **Figure 2D**. In the same figure, air has been entrapped within the fluidic channel during the injection of the crystallization solution, as can be seen in the upper-left part of the protein reservoir. **Figure 2E** is a close-up photograph of the protein reservoir after the manual deposition of the protein droplet with a pipette and before the encapsulation of the droplet with a piece of PMMA and Kapton tape, as described in steps 5.2 and 5.3 of the protocol. The microfluidic chip ready to be used for crystallization experiments, after the encapsulation of the protein sample and the gluing of the fluidic connectors, is depicted in **Figure 2C**. The air-tight assembly ensures that leakages cannot occur. The fluidic connectors for the inlet and outlet ports of the microfluidic channel can be either the commercially available ones as described in step 4.1 of the protocol and shown in **Figure 2C**, or disposable laboratory pipette tips can be used for the same purpose (**Figure 2B**, protocol step 4.4).

For the fabrication of the microfluidic chips, optically transparent and biologically inert materials were chosen, demonstrating high compatibility for in situ X-ray diffraction experiments at room temperature. The interactions of X-rays, absorption, and scattering, with the materials composing the microfluidic device and the surrounding atmosphere (air) generate a signal known as background noise. This noise sums up to the diffraction signal of the protein crystals recorded by the detector, decaying the signal-to-noise ratio and should be maintained as low as possible during X-ray diffraction data collection. We have evaluated the background noise generated by the materials comprising the protein reservoir, which is in the direct path of the X-ray beam. The protein reservoir consists of the RC dialysis membrane, the Kapton tape and two PMMA pieces, one used as a substrate for the microchip and one used for the encapsulation of the protein sample. The thickness of the PMMA is 2 x 175 µm, of the Kapton tape 20 µm, and the RC dialysis membrane is approximately 40 µm thick (**Figure 1L**). The total thickness of these layers is about 410 µm and the NOA 81 layer is not in the direct X-ray path. Apart from the thickness of the fabrication materials, their density is also crucial for measuring the background scattering noise, as X-ray scattering increases with the elemental atomic number. For this reason, helium flux (a feature provided at BM30A-FIP at ESRF) was used instead of air during the data collection for material characterization and for protein diffraction experiments. **Figure 3C** illustrates the background noise generated by the Kapton tape, the RC dialysis membrane, the PMMA sheet, and their assembly in helium atmosphere. Each material was exposed for 20 s to X-rays of 0.98 Å wavelength and the sample-detector distance was 200 mm. The experiments were performed at the BM30A-FIP beamline at ESRF, as explained in step 7 of the protocol. Diffuse rings attributed to the interactions of the X-ray beam with the materials can be distinguished for the Kapton tape at a resolution lower than 4 Å, the PMMA sheet between 4–8 Å, and the dialysis membrane between 4–5 Å resolution. The background

noise generated by the dialysis chip is mainly observed at a resolution lower than 6 Å that does not affect the treatment of high-resolution diffraction data of the large lysozyme crystals. The background scattering intensity as a function of the resolution for the microchip and the separate materials are shown elsewhere[19]. In the measurement presented in **Figure 3C**, the dialysis chip was empty of any solution (protein or precipitant solution) and the contribution of the presence of solution to the background noise has not been measured. The chips were mounted in front of the X-ray beam with a 3D-printed support (**Figure 3B**) designed for in situ diffraction experiments[19]. However, the same support with dimensions equal to the dimensions of a 96-well/SBS standard crystallization plate, can be used for performing 1 to 3 crystallization experiments concurrently, as it can hold up to 3 chips simultaneously (**Figure 3A**).

Experiments were conducted to evaluate the efficiency of the microfluidic devices for the on-chip crystallization of model soluble proteins with the microdialysis method. The fluidic channel was filled as described in step 4 of the protocol, while steps 5 and 6 described how to encapsulate the protein sample within the dedicated protein reservoir and how to set up the crystallization experiments. **Figure 4** shows lysozyme crystals grown at 293 K under 1.5 M sodium chloride (NaCl) with 0.1 M sodium acetate (CH_3COONa) pH 4.0 (A) and under 1 M NaCl, 0.1 M CH_3COONa pH 4.5 with 30% polyethylene glycol (PEG) 400 (B). The lyophilized lysozyme powder was dissolved in water to a final concentration of ~30 mg mL^{-1} or in 20 mM CH_3COONa pH 4.2 buffer to a final concentration of ~20 mg mL^{-1} for the experiments illustrated in **Figure 4A and B**, respectively. The volume of the protein sample in both experiments was about 0.3 µL and the MWCO of the RC dialysis membrane embedded within the microchips lies in the range of 6–8 kDa. The lysozyme crystals shown in **Figure 3A** grew within 1 h and the crystals in **Figure 3B** grew within 30 min from the onset of the experiment. The crystallization experiments were carried out under static conditions. However, it has been shown[19] that conducting the experiments under flowing conditions provides the possibility to dynamically exchange the crystallization conditions and study phase diagrams, verifying the reversibility of the microdialysis method.

In situ X-ray diffraction data from the lysozyme crystals shown in **Figure 4A** were collected to demonstrate the suitability of the dialysis chips for such experiments. The data collection was carried out at BM30A-FIP beamline (ESRF) at room temperature, as described in step 7.2.1 of the protocol. The microchips were mounted at the beamline with the aid of the 3D-printed support (**Figure 3B**) and complete X-ray diffraction data sets were collected from two single lysozyme crystals grown on-chip under the conditions given in the second line of **Table 1**. The observed reflections of the data sets were processed, indexed, and integrated using XDS[48] and the molecular replacement and refinement were accomplished using Phaser[49] and Phenix[52], respectively. The crystallographic statistics for the complete data set of each lysozyme crystal and for the merging of the two data sets are provided in **Table 2**. For the molecular replacement, the PDB entry 193L was used.

Electron density maps from a single lysozyme crystal and the merged data set of the two crystals have been obtained at 1.95 Å and 1.85 Å, respectively, and are illustrated in **Figure 5A and B**. Both electron density maps show detailed structural information that can be obtained

by in situ X-ray diffraction experiments conducted directly on the dialysis microchip at room temperature from a single crystal or from multiple crystals, rendering the chips compatible for in situ X-ray crystallography studies.

FIGURE AND TABLE LEGENDS:

Figure 1: Schematic illustration of the dialysis chip fabrication. (**A**) SU-8 resin is deposited on two silicon wafers and spin coated. (**B**) An SU-8 master is acquired after irradiating the photoresist with UV light through a photomask and developing the unexposed parts. (**C**) PDMS is dispensed upon the SU-8 masters and after being cured at 338 K for 1 h, (**D**) the 2 PDMS molds produced by replica molding and imprinting the micro-patterns are peeled of the masters and (**E**) cut to the appropriate size. (**F**) The PDMS molds are supported on a glass slide incorporating the RC dialysis membrane in between the two central pillars. (**G**) The 2 PDMS molds are then aligned and desiccated for ~30 min in a vacuum chamber. (**H**) The NOA 81 resin is poured in between the two molds and (**I**) fills the space by capillarity. (**J**) After the first exposure to UV light, the bottom PDMS mold is removed and the assembly is deposited on a PMMA sheet. (**K**) The second UV exposure follows in order to fully polymerize the NOA 81 resin and the dialysis chip is ready-to-use after removing the remaining upper PDMS mold. (**L**) Side view schematic of the dialysis chip where all the layers of the device and their respective thickness is indicated.

Figure 2: Dialysis chips embedding an RC dialysis membrane for on-chip protein crystallization and in situ X-ray diffraction experiments. (**A**) NOA 81 microchips on 175 µm thick PMMA substrate with a protein reservoir of 0.1 µL (left) and 0.3 µL (right) nominal volume. (**B**) Microchips with pipette tips as fluidic connectors glued on the inlet and outlet ports of the fluidic channel. (**C**) Picture of a microchip during a crystallization experiment. The protein sample is encapsulated with a piece of 175 µm thick PMMA sheet and Kapton tape. Peek Nanoport connectors are used for the inlet and outlet ports of the fluidic channel. (**D**) Top view of the protein reservoir during the circulation of the crystallization solution within the fluidic channel. Air is trapped in the upper part of the reservoir right under the RC dialysis membrane, which can be clearly detected. (**E**) Top view of the dialysis reservoir through an optical microscope during the deposition of the protein sample. The protein droplet is deposited right above the embedded RC dialysis membrane.

Figure 3: The 3D-printed support (**A**) for the microchips used during crystallization experiments and (**B**) mounted in front of the X-ray beam at BM30A-FIP beamline at the ESRF for in situ X-ray diffraction experiments. (**C**) Background noise generated by the interaction of X-rays with Kapton, RC dialysis membrane, PMMA, and the dialysis chip (from left to right).

Figure 4: On-chip crystallization of lysozyme with the microdialysis method. (**A**) Lysozyme (~30 mg mL^{-1}) crystals grown on-chip under 1.5 M NaCl and 0.1 M CH_3COONa pH 4.0 and (**B**) lysozyme (~20 mg mL^{-1}) crystals grown under crystallization conditions containing 1 M NaCl, 0.1 M CH_3COONa pH 4.5, and 30% PEG 400. Both experiments were conducted at 293 K.

Figure 5: Electron density maps of the refined lysozyme structure from (A) a single crystal and (B) the merged data set of two crystals grown on-chip via microdialysis. The maps were obtained at 1.95 Å and 1.84 Å, respectively, contoured at 1σ.

Table 1: Composition of the protein buffer and the precipitant solution for on-chip crystallization of lysozyme with the microdialysis method. The lysozyme crystals grown on-chip with the conditions provided in the second line were used for in situ X-ray diffraction data collection.

Table 2: Data collection parameters, crystallographic and refinement statistics of lysozyme crystals grown on-chip via the microdialysis method. Values provided in parentheses correspond to the highest resolution shell. The fourth column corresponds to values obtained after merging the data sets of the second and third column.

DISCUSSION:

A microfluidic device has been developed for on-chip protein crystallization with the microdialysis method and in situ X-ray diffraction experiments at room temperature. NOA 81 chips integrating RC dialysis membranes of any MWCO in order to use microdialysis for on-chip protein crystallization can be fabricated. Fabrication materials with a relatively high X-ray transparency were used, rendering the chips compatible for in situ protein crystallography. The fabrication materials that compose the compartment for protein crystallization of the device (PMMA, Kapton, RC dialysis membrane) were evaluated to generate low background noise. Specifically, the background noise generated by the dialysis chip is mainly observed at low resolution (>6 Å) and does not affect the treatment of high-resolution diffraction data of the large lysozyme crystals required for protein structure determination. The automation of the data collection is amplified using a 3D printed support that can be mounted directly in macromolecular crystallography beamlines and carry up to three microchips simultaneously. This way, manual harvesting and manipulation of the fragile protein crystals is avoided. Moreover, the data collection takes place at room temperature, avoiding the need for cryoprotection which can be related to conformational changes from the native protein structure[2,3].

The use of microdialysis as a method to grow crystals on-chip allows to accurately monitor and control the crystallization process. As discussed in the introduction, most of the conventional protein crystallization methods have been implemented using microfluidic devices[11,14]. However, the advantages of dialysis for protein crystallization had not yet been fully exploited at the microscale. On-chip microdialysis provides the possibility to study phase diagrams and perform screening and optimization of crystallization conditions with the same protein sample[19]. For the prototypes presented in this work, the protein consumption per chip is limited down to 0.1 or 0.3 µL. Based on the experimental work so far, the most critical steps of the protocol do not derive from the chips' fabrication procedure but from the crystallization process. The fabrication protocol includes many steps but it is straightforward and enables the fabrication of numerous devices (20 to 30 chips) in a single day in the clean room, with relatively inexpensive materials. However, the on-chip crystallization of proteins can be a

delicate procedure due to the intrinsic stochastic nature of nucleation and crystal growth, especially in the microscale. A case study has been described, where well-established conditions were used for the crystallization of lysozyme that yielded robust, well-defined crystals suitable for in situ X-ray diffraction data collection. Nevertheless, difficulties may arise by the use of more challenging protein targets, such as membrane proteins, where the crystallization medium is much more complicated, phase diagrams are not known and well-working crystallization conditions are not yet well established. The dialysis chip offers the possibility to surpass these difficulties and study phase diagrams on-chip, without disposing the valuable and frequently costly protein sample, by merely exchanging the crystallization solution within the microfluidic channel.

The versatility of the microfluidic devices stems from exploiting microdialysis for on-chip protein crystallization in order to reversibly control crystallization conditions and map concentration and temperature varied phase diagrams using low protein volume. Moreover, the device is compatible with in situ X-ray diffraction experiments and the prototyping of the devices is inexpensive and rapid. Numerous, isomorphous crystals of soluble and membrane proteins (in preparation) can be grown on-chip and it is expected that all these features can be utilized for serial X-ray crystallography studies of challenging protein targets at synchrotron and XFEL facilities. Finally, performing on-chip and in situ time-resolved studies is a future possibility that could be of significant interest to the crystallographic community. Therefore, by growing crystals on the dialysis chip and introducing the reagents into the microfluidic channel, either manually (using a syringe) or automatically (with a pressure-control fluid system or a syringe-pump), future efforts will focus on proving that the microfluidic chips can be successfully used to trigger time-resolved experiments on synchrotron beamlines.

ACKNOWLEDGMENTS:

MBS acknowledges the support of the MI / CNRS under the contract Instrumentation at the limits 2014–2015. NJ acknowledges CEA's International Doctoral Research Program (Irtelis) for the PhD Fellowship. MBS and SJ acknowledge funding from the European Union's Horizon 2020 Research and Innovation Programme under Marie Skłodowska-Curie grant agreement number 722687. MBS, SJ, and NJ thank LIPhy (UGA) for the clean room establishment for microfabrication experiments. IBS acknowledges integration into the Interdisciplinary Research Institute of Grenoble (IRIG, CEA).

DISCLOSURES:

The authors have nothing to disclose.

REFERENCES:

1. Garman, E. F. Radiation damage in macromolecular crystallography: what is it and why should we care? *Acta Crystallographica, Section D: Biological Crystallography*. **66**, 339–351 (2010).
2. Henderson, R. The potential and limitations of neutrons, electrons and X-rays for atomic resolution microscopy of unstained biological molecules. *Quarterly Reviews of Biophysics*. **28** (2), 171–193 (1995).

3. Fraser, J. S. et al. Accessing protein conformational ensembles using room-temperature X-ray crystallography. *Proceedings of the National Academy of Sciences of the United States of America*. **108** (39), 16247–16252 (2011).
4. Gotthard, G. et al. Specific radiation damage is a lesser concern at room temperature. *IUCrJ*. **6** (4), 665–680 (2019).
5. Martin-Garcia, J. M., Conrad, C. E., Coe, J., Roy-Chowdhury, S., Fromme, P. Serial femtosecond crystallography: A revolution in structural biology. *Archives of Biochemistry and Biophysics*. **602**, 32–47 (2016).
6. Gicquel, Y. et al. Microfluidic chips for in situ crystal X-ray diffraction and in situ dynamic light scattering for serial crystallography. *Journal of Visualized Experiments: JoVE*. **134**, e57133 (2018).
7. Chapman, H. N. et al. Femtosecond X-ray protein nanocrystallography. *Nature*. **470**, 73–78 (2011).
8. Hunter, M. S. et al. Fixed-target protein serial microcrystallography with an x-ray free electron laser. *Science Reports*. **4**, 6026 (2015).
9. Pawate, A. S. et al. Towards time-resolved serial crystallography in a microfluidic device. *Acta Crystallographica, Section F: Structural Biology Communications*. **71**, 823–830 (2015).
10. Owen, R. L. et al. Low-dose fixed-target serial synchrotron crystallography. *Acta Crystallographica, Section D: Structural Biology*. **73**, 373–378 (2017).
11. Leng, J., Salmon, J.-B. Microfluidic crystallization. *Lab on a Chip*. **9**, 24–34 (2009).
12. Morel, M., Galas, J.-C., Dahan, M., Studer, V. Concentration landscape generators for shear free dynamic chemical stimulation. *Lab on a Chip*. **12**, 1340–1346 (2012).
13. Miralles, V., Huerre, A., Malloggi, F., Jullien, M.-C. A review of heating and temperature control in microfluidic systems: techniques and applications. *Diagnostics*. **3**, 33–67 (2013).
14. Sui, S., Perry, S. L. Microfluidics: from crystallization to serial time-resolved crystallography. *Structural Dynamics*. **4**, 032202 (2017).
15. Hansen, C. L., Sommer, M. O. A., Quake, S. R. Systematic investigation of protein phase behavior with a microfluidic formulator. *Proceedings of the National Academy of Sciences of the United States of America*. **101** (40), 14431–14436 (2004).
16. Laval., P., Lisai, N., Salmon, J.-B., Joanicot, M. A microfluidic device based on droplet storage for screening solubility diagrams. *Lab on a Chip*. **7**, 829–834 (2007).
17. Shim, J.-Uk et al. Control and measurement of the phase behavior of aqueous solutions using microfluidics. *Journal of the American Chemical Society*. **129**, 8825–8835 (2007).
18. Selimovic, S., Gobeaux, F., Fraden, S. Mapping and manipulating temperature–concentration phase diagrams using microfluidics. *Lab on a Chip*. **10**, 1696–1699 (2010).
19. Junius, N. et al. A microfluidic device for both on-chip dialysis protein crystallization and in situ X-ray diffraction. *Lab on a Chip*. **20**, 296–310 (2020).
20. Greaves, E. D., Manz, A. Towards on-chip X-ray analysis. *Lab on a Chip*. **5**, 382–391 (2005).
21. Dhouib, K. et al. Microfluidic chips for the crystallization of biomacromolecules by counter-diffusion and on-chip crystal X-ray analysis. *Lab on a Chip*. **9**, 1412–1421 (2009).
22. Guha, S., Perry, S. L., Pawate, A. S., Kenis, P. J. A. Fabrication of X-ray compatible microfluidic platforms for protein crystallization. *Sensors and Actuators B. Chemical*. **174**, 1–9 (2012).

23. Sui, S. et al. Graphene-based microfluidics for serial crystallography. *Lab on a Chip*. **16**, 3082–3096 (2016).
24. Russo Krauss, I., Merlino, A., Vergara, A., Sica, F. An overview of biological macromolecule crystallization. *International Journal of Molecular Science*. **14**, 11643–11691 (2013).
25. McPherson, A., Gavira, J. A. Introduction to protein crystallization. *Acta Crystallographica, Section F: Structural Biology and Crystallization Communications*. **70**, 2–20 (2014).
26. Zheng, B., Tice, J. D., Roach, L. S., Ismagilov, R. F. A droplet-based, composite PDMS/Glass capillary microfluidic system for evaluating protein crystallization conditions by microbatch and vapor-diffusion methods with on-chip X-ray diffraction. *Angewandte Chemie (International Ed*ition in English) **43**, 2508–2511 (2004).
27. Talreja, S., Kim, D. Y., Mirarefi, A. Y., Zukoski, C. F., Kenis, P. J. A. Screening and optimization of protein crystallization conditions through gradual evaporation using anovel crystallization platform. *Journal of Applied Crystallography*. **38**, 988–995 (2005).
28. Hansen, C. L., Classen, S., Berger, J. M., Quake, S. R. A microfluidic device for kinetic optimization of protein crystallization and in situ structure determination. *Journal of American Chemical Society*. **128**, 3142–3143 (2006).
29. Schieferstein, J. M. et al. X-ray Transparent microfluidic platforms for membrane protein crystallization with microseeds. *Lab on a Chip*. **18**, 944–954 (2018).
30. Ghazal, A. et al. Recent advances in X-ray compatible microfluidics for applications in soft materials and life sciences. *Lab on a Chip*. **16**, 4263–4295 (2016).
31. Li, L., Ismagilov, R. F. Protein crystallization using microfluidic technologies based on valves, droplets, and SlipChip. *Annual Review of Biophysics*. **39**, 139–158 (2010).
32. Du, W., Li, L., Nichols, K. P., Ismagilov, R. F. SlipChip. *Lab on a Chip*. **9**, 2286–2292 (2009).
33. Zhang, S. et al. Microfluidic platform for optimization of crystallization conditions. *Journal of Crystal Growth*. **472**, 18–28 (2017).
34. Abdallah, B. G. et al. Protein crystallization in an actuated microfluidic nanowell device. *Crystal Growth & Design*. **16**, 2074–2082 (2016).
35. Monteiro, D. C. F. et al. A microfluidic flow-focusing device for low sample consumption serial synchrotron crystallography experiments in liquid flow. *Journal of Synchrotron Radiation*. **26**, 406–412 (2019).
36. de Wijn, R. et al. A simple and versatile microfluidic device for efficient biomacromolecule crystallization and structural analysis by serial crystallography. *IUCrJ*. **6**, 454–464 (2019).
37. Shim, J.-Uk, Cristobal, G., Link, D. R., Thorsen, T., Fraden, S. Using microfluidics to decouple nucleation and growth of protein crystals. *Crystal Growth & Design*. **7**, 2192–2194 (2007).
38. de Jong, J., Lammertink, R. G. H., Wessling, M. Membranes and microfluidics: a review. *Lab on a Chip*. **6**, 1125–1139 (2006).
39. Paustian, J. S., Nery Azevedo, R., Lundin, S.-T. B., Gilkey, M. J., Squires, T. M. Microfluidic microdialysis: spatiotemporal control over solution microenvironments using integrated hydrogel membrane microwindows. *Physical Review X*. **3**, 041010 (2013).
40. Kornreich, M., Heymann, M., Fraden, S., Beck, R. Cross polarization compatible dialysis

chip. *Lab on a Chip*. **14**, 3700–3704 (2014).
41. Song, S., Singh, A. K., Shepodd, T. J., Kirby, B. J. Microchip dialysis of proteins using in situ photopatterned nanoporous polymer membranes. *Analytical Chemistry*. **76**, 2367–2373 (2004).
42. Skou, M., Skou, S., Jensen, T. G., Vestergaard, B., Gillilan, R. E. In situ microfluidic dialysis for biological small-angle X-ray scattering. *Journal of Applied Crystallography*. **47**, 1355–1366 (2014).
43. Zou, L. et al. A multistage dialysis microdevice for extraction of cryoprotectants. *Biomedical Microdevices*. **19**, 30 (2017).
44. Satya Eswari, J., Naik, S. A critical analysis on various technologies and functionalized materials for manufacturing dialysis membranes. *Materials Science for Energy Technologies*. **3**, 116–126 (2020).
45. Spano, M., Salmon, J.-B., Junius, N. FR3044685A1, UJF, 2015.
46. Bartolo, D., Degre, G., Nghe, P., Studer, V. Microfluidic stickers. *Lab on a Chip*. **8**, 274–279 (2008).
47. Junius, N. et al. A crystallization apparatus for temperature controlled flow-cell dialysis with real-time visualization. *Journal of Applied Crystallography*. **49**, 806–813 (2016).
48. Kabsch, W. XDS. *Acta Crystallographica, Section D: Biological Crystallography*. **66**, 125–132 (2010).
49. Winn, M.D. et al. Overview of the CCP4 suite and current developments. *Acta Crystallographica, Section D: Biological Crystallography*. **67**, 235–242 (2011).
50. Emsley, P., Lohkamp, B., Scott, W. G., Cowtan, K. Features and developments of COOT. *Acta Crystallographica, Section D: Biological Crystallography*. **66**, 486–501 (2010).
51. Apostolopoulou, V., Junius, N., Sear, R. P., Budayova-Spano, M. Mixing salts and polyethylene glycol into protein solutions: The effects of diffusion across semipermeable membranes and of convection. *Crystal Growth & Design*. **20**, 3927–3936 (2020).
52. Liebschner, D. et al. Macromolecular structure determination using X-rays, neutrons and electrons: recent developments in *Phenix*. *Acta Crystallographica, Section D: Structural Biology*. **75**, 861–877 (2019).
53. Xia, Y., Whitesides, G.M. Soft Lithography. *Annual Review of Materials Science*. **28**, 153–84 (1998).
54. Nogly, P. et al. Lipidic cubic phase injector is a viable crystal delivery system for time-resolved serial crystallography. *Nature Communications*. **7**, 12314 (2016).
55. Baxter, E. L. et al. High-density grids for efficient data collection from multiple crystals. *Acta Crystallographica, Section D: Structural Biology*. **72**, 2–11 (2016).
56. Feiler, C. G., Wallacher, D., Weiss, M. S. An all-in-one sample holder for macromolecular X-ray crystallography with minimal background scattering. *Journal of Visualized Experiments*. **149**, e59722 (2019).

Figure 1

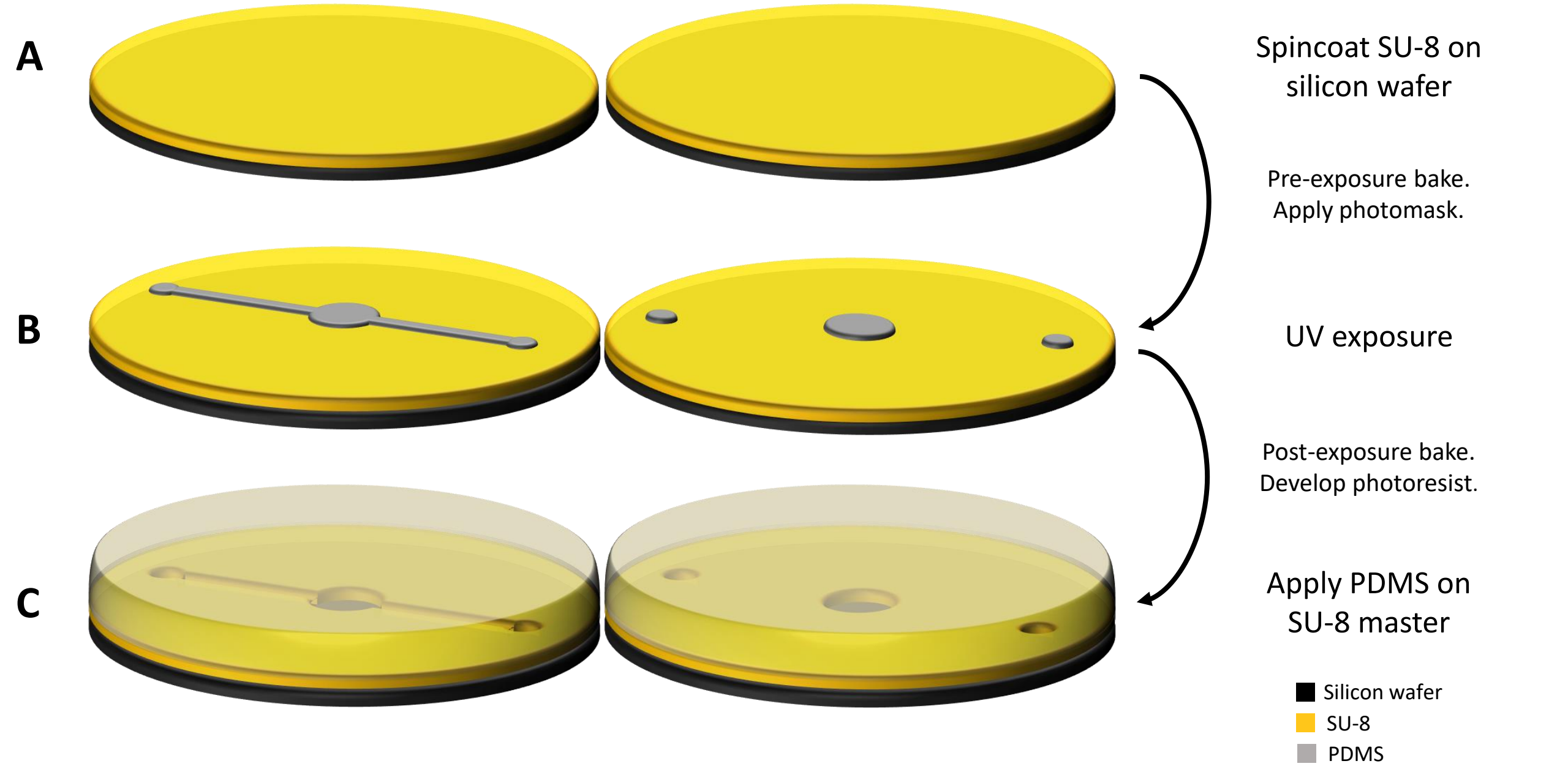

D

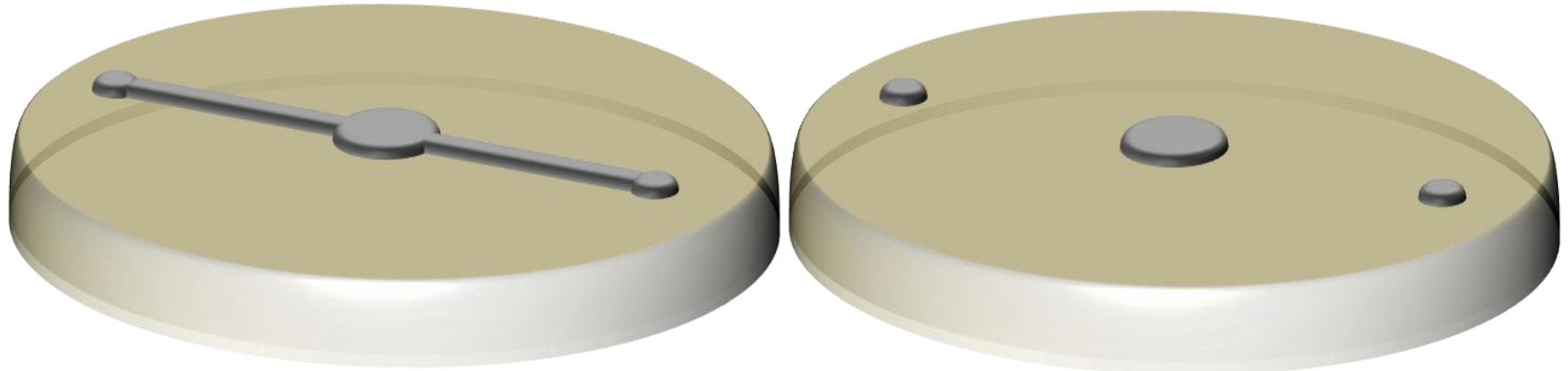

Peel of PDMS molds from SU-8 master

E

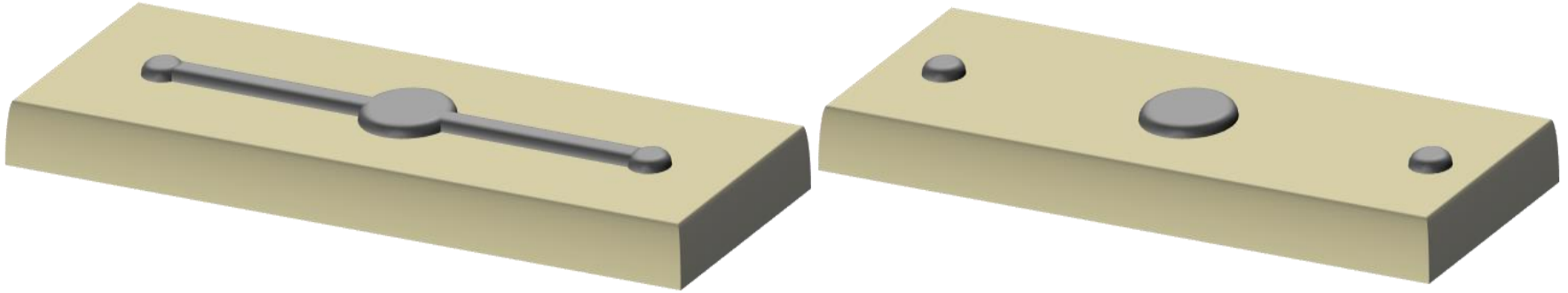

Cut PDMS molds

F

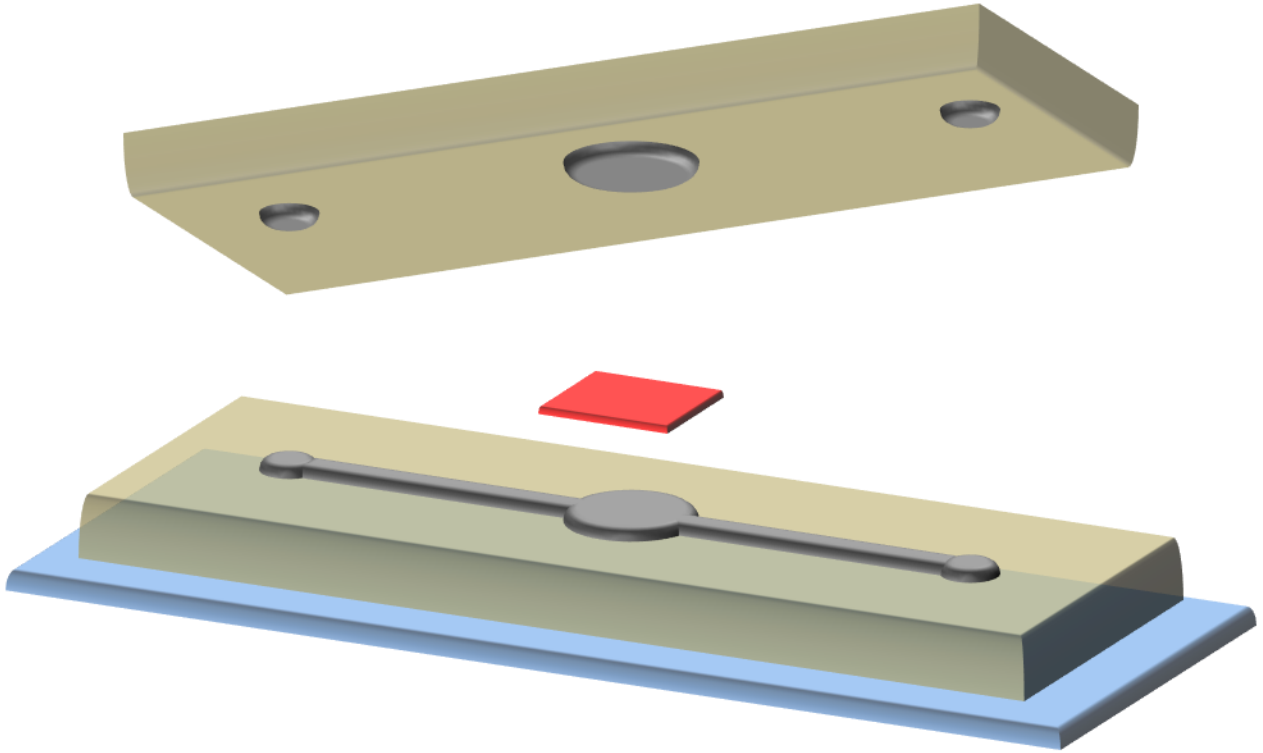

Deposit PDMS molds on glass slide. Cut and place RC dialysis membrane in between the central pillars.

G

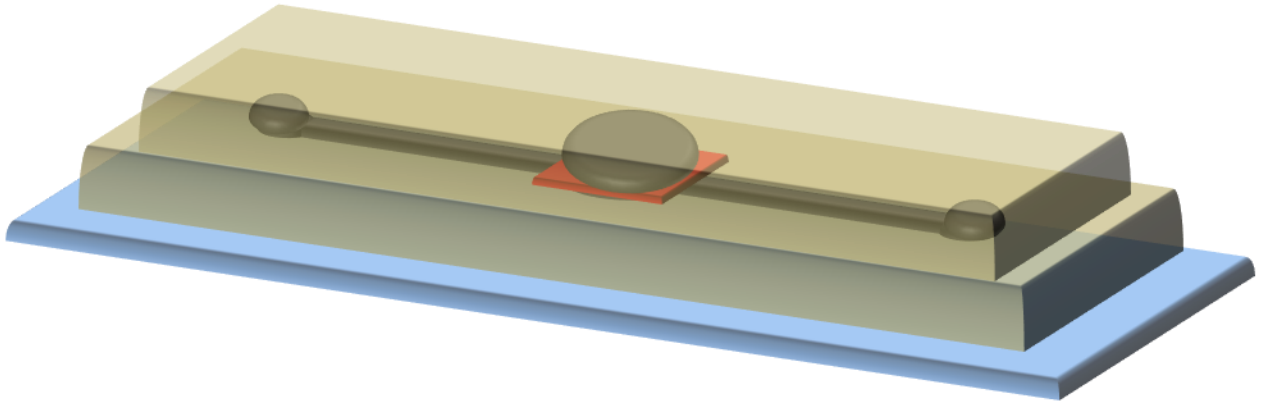

Align and desiccate in vacuum chamber.

Glass slide

RC membrane

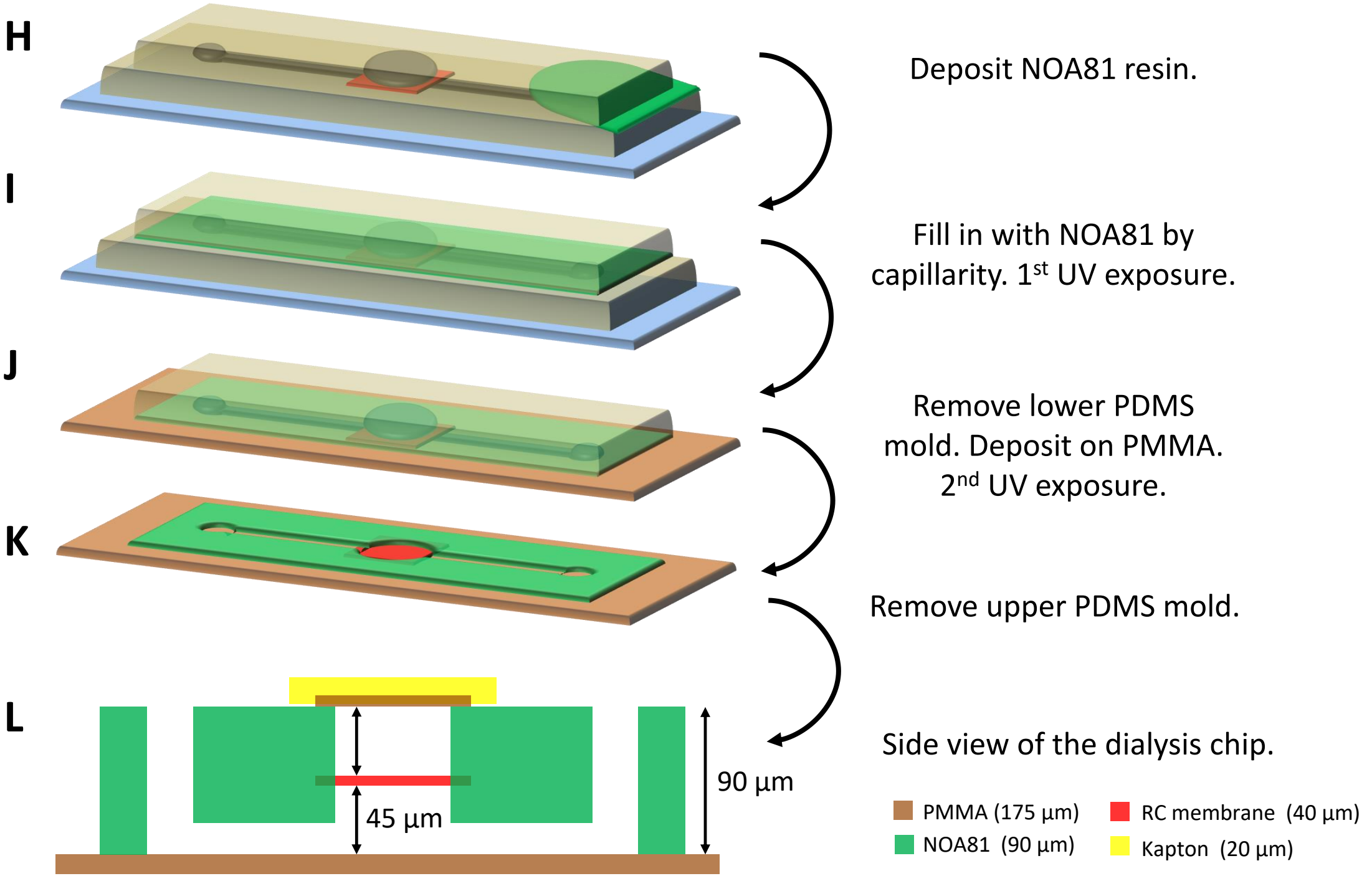
H
I
J
K
L
Deposit NOA81 resin.
Fill in with NOA81 by capillarity. 1st UV exposure.
Remove lower PDMS mold. Deposit on PMMA. 2nd UV exposure.
Remove upper PDMS mold.
Side view of the dialysis chip.
90 µm
45 µm
PMMA (175 µm)
NOA81 (90 µm)
RC membrane (40 µm)
Kapton (20 µm)

Figure 2

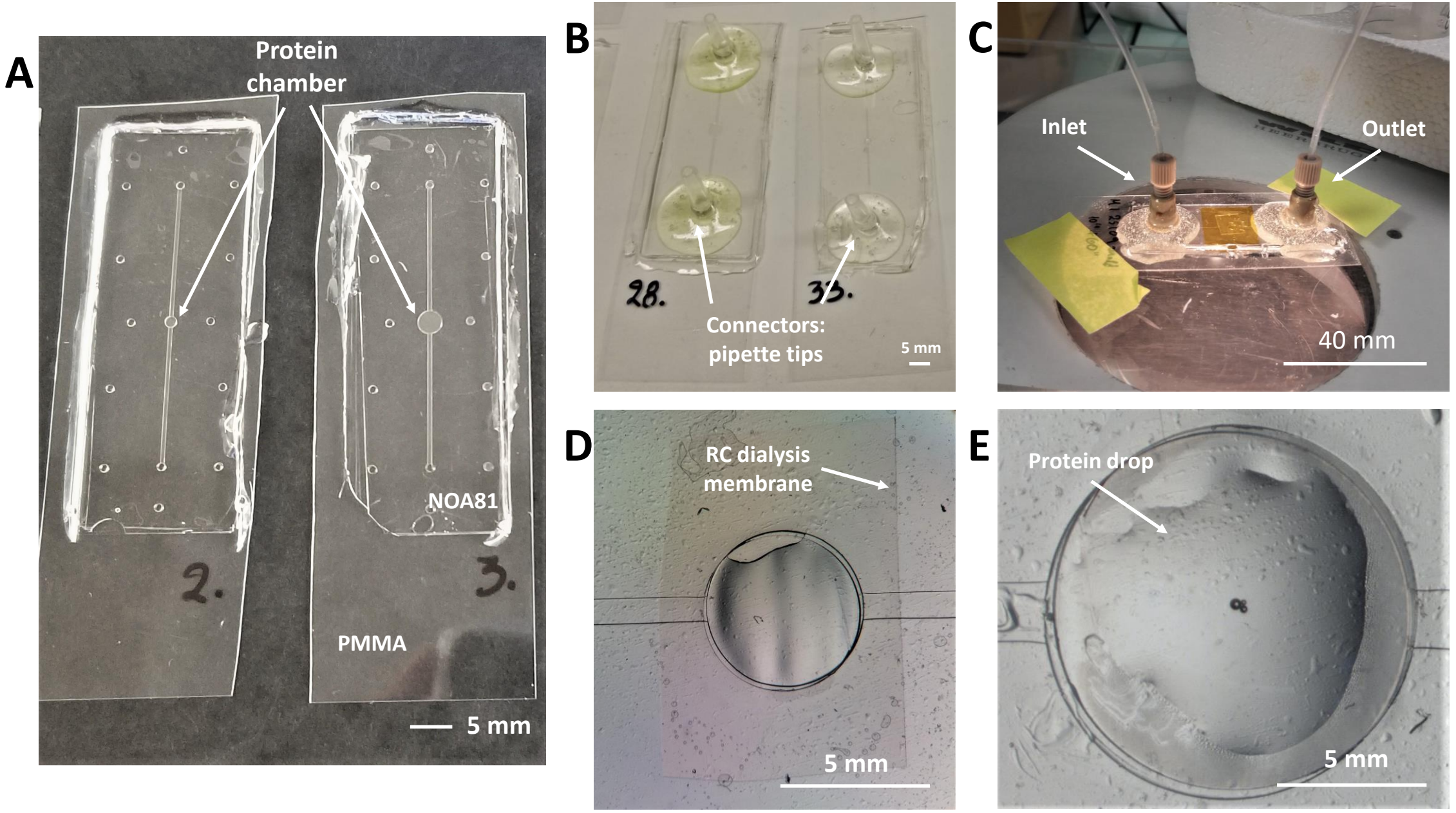

Figure 3

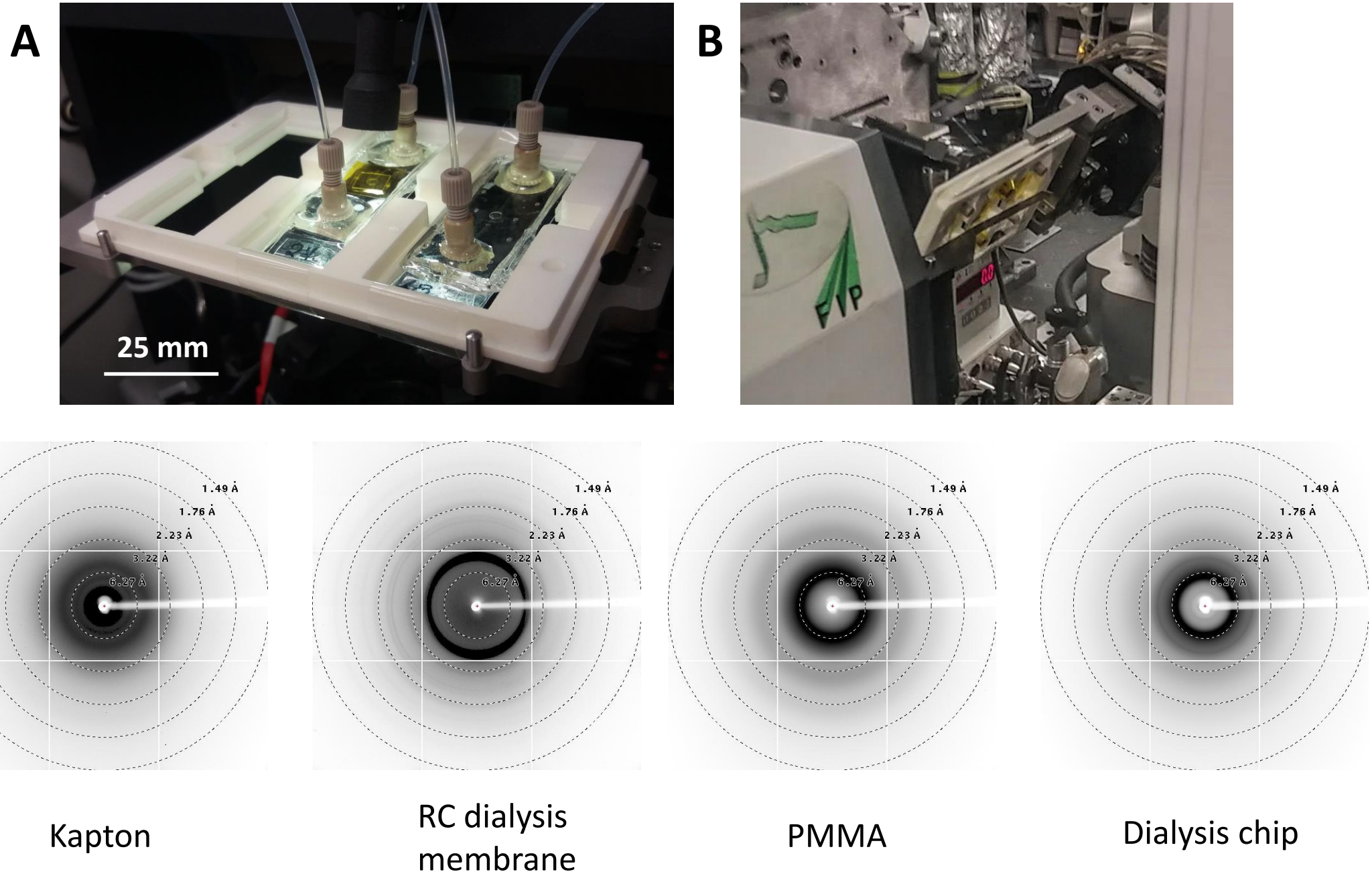

Figure 4

Click here to access/download;Figure;Figure 4.pdf

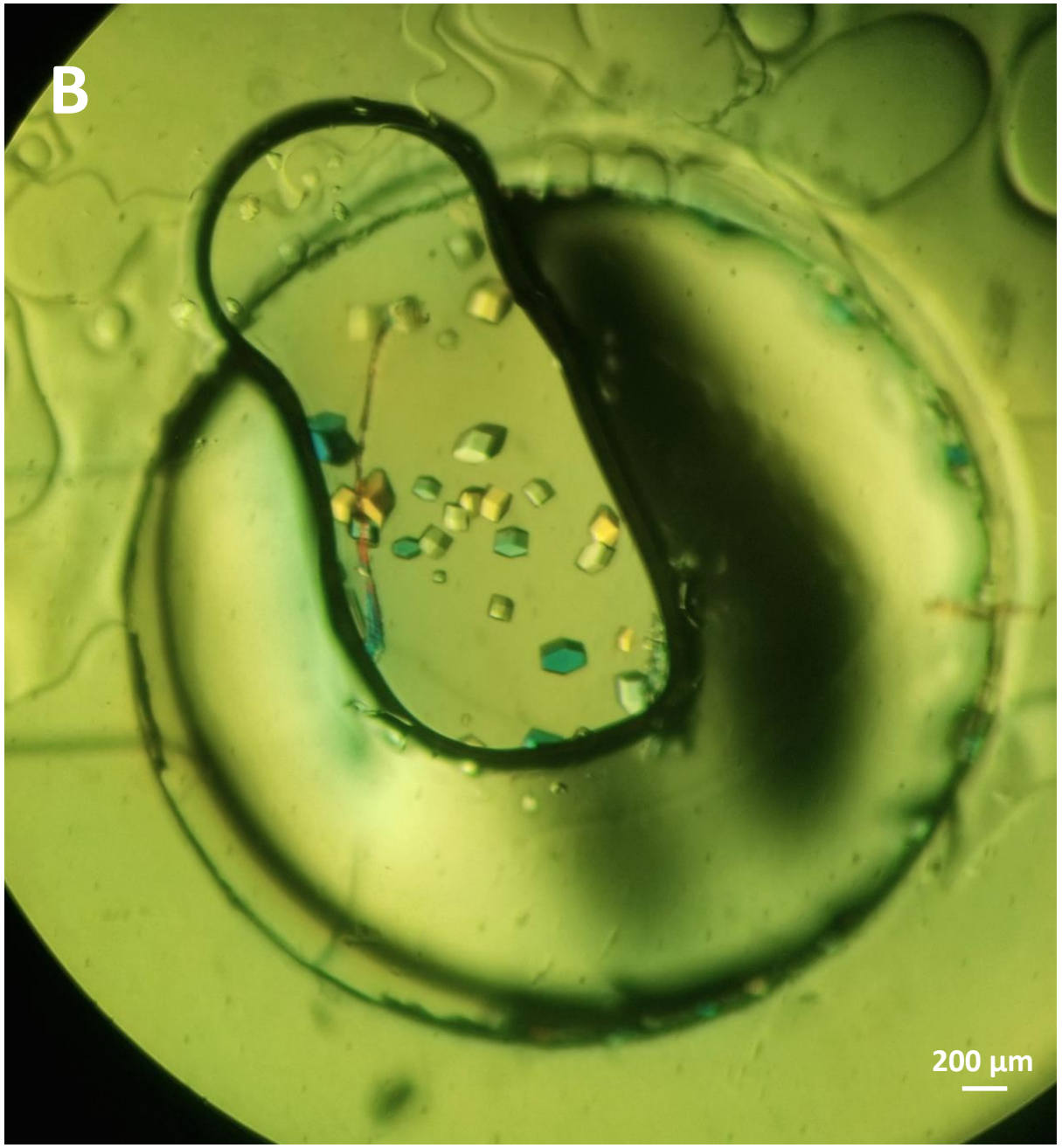

Figure 5

Click here to access/download;Figure;Figure 5.pdf

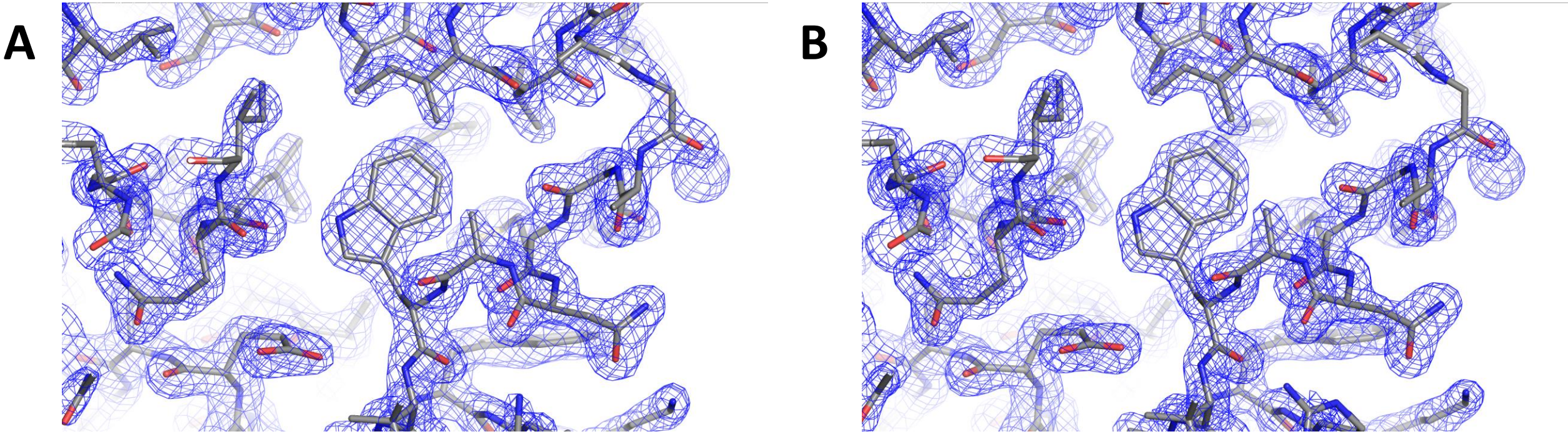

Table 1

Protein	Protein concentration (mg mL^{-1})	Protein bufffer
Lysozyme	~ 30	Water
Lysozyme	~ 20	20 mM CH3COONa pH 4.2

Initial concentration of precipitant solution	MWCO of RC dialysis membrane (kDa)	Temperature (K)
1.5 M NaCl 0.1 M CH3COONa pH 4.0	12 - 14	293
1 M NaCl 0.1 M CH3COONa pH 4.5 30% PEG 400	12 - 14	293

Table 2

Protein	Lysozyme	Lysozyme	Lysozyme
Number of crystals	1	1	2
Number of diffraction frames	40	30	70
Oscillation (°) per exposure	1	1	
Exposure time (s)	30	30	
Temperature (K)	293	293	293
Space group	$P4_32_12$	$P4_32_12$	$P4_32_12$
Unit cell parameters	78.86 78.86 37.87 90.0 90.0 90.0	79.17 79.17 37.95 90.0 90.0 90.0	78.47 78.47 37.65 90.0 90.0 90.0
Resolution range (Å)	27.31 - 1.95 (2.02 - 1.95)	27.39 - 1.96 (2.03 - 1.96)	27.17 - 1.85 (1.91 - 1.85)
Mosaicity (°)	0.319	0.121	
Total reflections (observed)	25127 (3552)	19991 (3001)	
Unique reflections (observed)	8641 (1357)	8295 (1321)	10404 (975)
Redudancy	2.90 (2.61)	2.41 (2.27)	
Completeness (%)	95.0 (94.8)	91.9 (93.3)	98.23 (93.15)
Mean I/σ	6.83 (1.16)	7.09 (1.66)	3.7
$CC_{(1/2)}$	99.1 (42.4)	97.9 (37.0)	97.0
R-merge			0.184
R-meas	0.139	0.221	0.219
R-pim			0.116
Reflections used in refinement	8645 (787)	8451 (857)	10391 (965)
Reflections used for R-free	864 (78)	846 (85)	1039 (96)
R-work	0.1988 (0.2968)	0.1853 (0.2872)	0.1839 (0.3102)
R-free	0.2430 (0.3437)	0.2297 (0.3622)	0.2207 (0.3703)
Number of non-hydrogen atoms	1069	1071	1096
macromolecules	1012	1012	1012
water	55	57	82
ligand	2	2	2
Protein residues	131	131	131
Rms (bonds, Å)	0.008	0.009	0.005
Rms (angles, °)	1.17	1.26	1.05
Ramachandran favored (%)	98.43	97.64	99.21
Ramachandran allowed (%)	1.57	2.36	0.79
Ramachandran outliers (%)	0.00	0.00	0.00
Avegare B-factor	34.26	28.54	24.34
protein	33.94	28.14	23.62
water	40.23	35.57	33.16
ligands	33.23	29.63	24.77

Name of Material/Equipment	Company	Catalog Number	Comments/Description
3 in wafer	Silicon Materials Inc.		Silicon wafer
Centrifuge	Eppendorf	Minispin	Bench-top centrifuge
CleWin 3.0	WieWeb software		Designing software
Epoxy glue	Devcon		5 minutes epoxy glue
Fluidic connectors	Cluzeau Info Lab	N-333	NanoPort kit for 1/16" OD tubing
Hen egg-white lysozyme	Roche	10 837 059 001	Lyophilized protein powder
High-vacuum silicone grease	Sigma-Aldrich	Z273554	Dow Corning high-vacuum silicone grease
HMDS	Sigma-Aldrich	440191	Silane, chemical
Hot plate	Sawatec	HP-200-Z-HMDS BM	Hot plate
Isopropyl alcohol	Sigma-Aldrich		Solvent
Kapton tape	DuPont		Polyimide tape
Mask aligner	SUSS MicroTec	MJB4	Mask aligner, UV source
Membrane filter	Millipore	GSWP04700	0.22 µm pore size filter
Microscope glass slide	Fisher Scientific	12164682	3 x 1 in glass slides
NOA81	Norland Products Inc.	NOA81	Photocurable resin
Oven	Memmert		Oven
Parafilm	Sigma-Aldrich	P6543	Parafilm M roll size 20 in. × 50 ft
PDMS	Dow Corning	Sylgard 184	Silicone
PEG 400	Hampton Research	HR2-603	Chemical
Petri dish	Sigma-Aldrich	P5731	100 x 15 mm
PGMEA	Sigma-Aldrich	484431	Developer
Plasma equipment	Diener Electronic	ZEPTO	Plasma treatment
PMMA	Goodfellow	137-745-63	PMMA sheets 150x150 mm, 0.175 mm thickness
Pressure driven system	Elveflow	OB1 MK3+	Pressure/vacuum controller
PTFE tubing	Elveflow/Darwin microfluidics	LVF-KTU-15	PTFE tubing roll 1/16" OD X 1/32" ID

RC dialysis membrane	Spectra/Por		Various MWCOs
Scalpel	Swann-Morton		Carbon steel surgical blades
Sodium acetate	Sigma-Aldrich	S2889	Chemical
Sodium chloride	Sigma-Aldrich	746398	Chemical
Solidworks	Dassault Systemes		3D-CAD designing software
Spin coater	SPS	Spin150	Wafer spinner
SU-8 3000 series	MicroChem Corp.	SU-8 3050	Photoresist
Syringe	BD	309628	1 mL Luer-Lok syringe
UV crosslinker	Uvitec	CL-508	UV crosslinker

Crystallization of proteins on chip by microdialysis for *in situ* X-ray diffraction studies

Sofia Jaho[1], Niels Junius[1,*], Franck Borel[1], Yoann Sallaz-Damaz[1], Jean-Baptiste Salmon[2] and Monika Budayova-Spano[1]

[1] Université Grenoble Alpes, CEA, CNRS, IBS, Grenoble, France

[2] CNRS, Solvay LOF, UMR 5258, Université Bordeaux, Pessac, France

[*] Current address: Elvesys, 172 Rue de Charonne, 75011 Paris, France

Response to editorial, production and reviewers' comments:

Journal of Visualized Experiments – JoVE61660R1

Dear Editor,

We first thank all referees for their careful reading of our manuscript, their valuable remarks and for their relevant comments regarding our work. We are also pleased to read that most referees considered our protocol was clearly described, understood and worthy of publication. We list below our responses to all the points raised by the editorial and production team and by the referees, as well as the changes made to our revised manuscript (highlighted below in red and with the same colour in the revised version of the manuscript). We now hope that this revised and improved version of the manuscript as well as the video can be published in the Journal of Visualized Experiments as the video produced by the author.

Editorial and production comments:
Changes to be made by the Author(s) regarding the written manuscript:
1. Please take this opportunity to thoroughly proofread the manuscript to ensure that there are no spelling or grammar issues.
2. Please revise the text to avoid the use of any personal pronouns (e.g., "we", "you", "our" etc.).
3. Please provide examples volumes and concentrations in the protocol so that a specific experiment can be presented in addition to the generalized one.
4. Please sort the Table of Materials alphabetically.

We have proofread the manuscript and personal pronouns have been removed. Specific experimental conditions have been provided and the Table of Materials has been sorted alphabetically.

Changes to be made by the Author(s) regarding the video:
1. The audio is too loud. Please reduce the volume by 3 to 6 dB.
2. 00:02-01:27 After the title card, the Introduction audio is good, but consider adding some visuals to help illustrate what is being talked about and also to help with audience engagement.

3. 11:34-12:36 Same issue with the Conclusion. Consider adding some graphics or illustrations while you wrap up.

The video has been revised according to the indications. The volume of the audio has been reduced by 6 dB.

Reviewer #1

Manuscript Summary:

This manuscript describes the fabrication and use of microfluidic in situ crystallization and data collection devices. The devices comprise a dialysis membrane separating the central chamber in two cavity, where crystallization trials using the microdialysis method can be performed. The chambers walls are made of X-ray compatible materials allowing in situ crystallographic data collection. Crystallization of lysozyme under two different conditions are demonstrated.

The presentation is in general clear and useful.

Major Concerns:

The manuscripts claims low background data collection (video 00:17), however there is not sufficient evidence on this point. Instead of the patterns in fig 3C, background curves must be presented as powder patterns on the same graph, for efficient comparison and assessing the background at high resolution. A comparison with background signal from another RT delivery mode would be most useful to demonstrate this. If I understand properly, the device thickness is 2x175 um PMMA, 2x50 um mother liquor or crystal, 20 um kapton, and the RC membrane (of unknown thickness?). This is probably not going to give a particularly low background, compared to other current RT delivery methods such as injectors (example doi 10.1038/ncomms12314), multicrystal grids (doi 10.1107/S2059798315020847) or XtalTool holders (doi: 10.3791/59722). Certainly, design optimization could help reducing the thickness (this could be discussed as well in the paper). Concerning this manuscript, I would suggest removing the claim of low background and stay by X-rays data collection compatibility as in many places of the text, which is already very useful since there are not many options for in situ data collection after microdialysis crystallization.

We would like to thank the reviewer for this very useful comment and the relevant references. Indeed, the claim of low background noise might be inadequate compared to other devices or strategies that have been developed for room temperature *in situ* X-ray diffraction studies. For example, Nogly *et al.* (reference 54) used a lipidic cubic phase (LCP) injector in order to study the structure of the light-driven photon pump bacteriorhodopsin (bR) by serial femtosecond crystallography (SFX) using an XFEL source. Specifically, the authors used a pump-probe approach with a temporal delay of 1 ms to investigate the protein's dynamics by implementing time-resolved serial femtosecond crystallography (TR-SFX). The crystal structure of bR was solved to 2.3 Å resolution, demonstrating the compatibility of an LCP injector for TR-SFX experiments with a reduced sample consumption (approximately 1 mg per collected time point). Another device compatible for room temperature *in situ* X-ray crystallography was developed by Baxter *et al.* (reference 55). The device is a high-density multi-crystal grid fabricated by a 100 or 200 µm thick polycarbonate plastic with laser-cut holes of various sizes. An additional 5 µm thick polycarbonate film can be fixed to one side of the grid when using the device for sitting- or hanging-drop crystallization experiments. This

high-density grid can be used in multiple ways as crystals can be loaded directly onto the ports of the device or crystals can be grown on the device by vapor diffusion or the LCP method using appropriate adaptors and incubation chambers. Moreover, the grid can be adjusted in a standard magnetic base with epoxy and can be used for *in situ* X-ray data collection at cryogenic or room temperature conditions in standard goniometer-based beamlines at synchrotron and XFEL facilities. The light-sensitive photosystem II (PSII) protein crystals tested for room temperature diffraction in the dark with the rastering method yielded a diffraction better than 2.5 Å resolution. More recently, Feiler *et al.* (reference 56) developed a sample holder (XtalTool) for macromolecular *in situ* X-ray crystallography at cryogenic and ambient temperature with minimal background noise contribution. Specifically, the holder comprises of a plastic support, a transparent COC foil and a microporous structured polyimide foil. It was designed to replace the commonly used cover slides for setting up crystallization drops, while it allows in-place manipulation such as ligand soaking, complex formation and cryogenic protection without opening the crystallization drop or manually handling the crystals. Moreover, the sample holder can be removed from the crystallization plate and placed onto a magnetic base for *in situ* data collection at standard goniometer-based beamlines. For ambient temperature data collection, the COC foil is removed prior to the experiment and only the 21 µm-thick polyimide foil contributes to background scattering, which in this case is minimal.

Several microfluidic devices have been developed for *in situ* X-ray diffraction experiments at room temperature and various fabrication materials have been assessed for their background scattering contribution (as discussed in lines 114-121). The choice of the fabrication materials, as well as, their thickness are indeed crucial to the generated background noise which leads to a degradation of the signal-to-noise ratio during data collection. We have chosen materials commonly used for microfluidic devices (PMMA, Kapton) and we have evaluated their background contribution. The diffuse rings are generated by PMMA between 4-8 Å resolution and by Kapton at a resolution lower than 4 Å. The respective noise generated by the regenerated cellulose (RC) dialysis membrane is observed at a resolution lower than 6 Å. These are the only materials of the dialysis chip that are located in the direct path of the X-ray beam, as the NOA 81 resin is not a part of the protein chamber. In a previous study (reference 19), we presented curves of the background scattering intensity of each material separately (Kapton tape, RC membrane, 175 µm-thick PMMA) and the microchip as a function of resolution (in Å). Scattering peaks can be distinguished for all the fabrication materials in the same resolution range where the diffuse rings are observed in Figure 3C. Concerning the thickness of the materials in the direct path of the X-ray beam, we would like to point out that the total thickness is 410 µm as stated in the manuscript. However, we apologize that it is not very clear how we reached to this calculation. The thickness of the PMMA is 2 x 175 µm (PMMA is used as a substrate for the chip and a small piece is used for the closure of the protein chamber), of the Kapton tape 20 µm and the RC dialysis membrane is approximately 40 µm thick. The last image (dialysis chip) in Figure 3C corresponds to the background noise generated only by these three materials with a total thickness of 410 µm. In the measurement presented in this figure, the dialysis chip was empty of any solution (protein or precipitant solution) and the contribution of the presence of solution to the background noise has not been measured. We recognize that for *in situ* diffraction data collection of Lysozyme crystals, the diffraction quality was not severely impacted, as we could eventually generate the electron density map at a relatively high resolution (close to 2 Å). However, we will keep in mind for future diffraction studies of more challenging protein targets that the background contribution of the protein solution (in the protein chamber with a height of 45 µm) and the precipitant solution (in the fluidic channel with a height of 45 µm) should be evaluated. We kindly thank the reviewer for this very useful remark.

The microfluidic chips presented in this work, are compatible for on-chip protein crystallization with the microdialysis method and *in situ* X-ray diffraction experiments at room temperature. In order to further lower the background noise generated by the microchips, optimization concerning the choice of the fabrication materials and their thickness could be implemented in future versions of the device. In this manuscript and video, we would like to emphasize the compatibility of the dialysis microchip with room temperature *in situ* diffraction data collection. Addressing the concerns posed by the reviewer, we made the following modifications in the manuscript and the video:

Manuscript lines 121 – 143:

Room temperature, *in situ* data collection has also been implemented in various delivery methods and devices. For example, Nogly *et al.*[54] used a lipidic cubic phase (LCP) injector in order to study the structure of the light-driven photon pump bacteriorhodopsin (bR) by serial femtosecond crystallography (SFX) using an XFEL source. The crystal structure of bR was solved to 2.3 Å resolution, demonstrating the compatibility of an LCP injector with time-resolved serial femtosecond crystallography (TR-SFX). Baxter *et al.*[55] designed a high-density multi-crystal grid, fabricated by a 100 or 200 µm thick polycarbonate plastic with laser-cut holes of various sizes. An additional 5 µm thick polycarbonate film can be fixed to one side of the grid when using the device for sitting- or hanging-drop crystallization experiments. This high-density grid can be used in multiple ways as crystals can be loaded directly onto the ports of the device or crystals can be grown on the device by vapor diffusion or the LCP method. Moreover, the grid can be adjusted in a standard magnetic base and used for *in situ* X-ray data collection at cryogenic or room temperature conditions. More recently, Feiler *et al.*[56] developed a sample holder for macromolecular *in situ* X-ray crystallography at cryogenic and ambient temperature with minimal background noise contribution. Specifically, the holder comprises of a plastic support, a transparent COC foil and a microporous structured polyimide foil. It was designed to replace the commonly used cover slides for setting up crystallization drops, while it allows in-place manipulation such as ligand soaking, complex formation and cryogenic protection without opening the crystallization drop or manually handling the crystals. Moreover, the sample holder can be removed from the crystallization plate and placed onto a magnetic base for *in situ* data collection at standard goniometer-based beamlines. For ambient temperature data collection, the COC foil is removed prior to the experiment and only the 21 µm-thick polyimide foil contributes to background scattering, which in this case is minimal.

Manuscript lines 574 – 575:

The thickness of the PMMA is 2 x 175 µm, of the Kapton tape 20 µm and the RC dialysis membrane is approximately 40 µm thick (Figure 1L).

Manuscript lines 591 – 593:

In the measurement presented in Figure 3C, the dialysis chip was empty of any solution (protein or precipitant solution) and the contribution of the presence of solution to the background noise has not been measured.

Video 00:17: The audio part has been modified accordingly.

A side-view schematic of the device throughout fabrication and device filling, all the way until X-ray data collection should be added for clarity. The relevant thicknesses need to be indicated on this schematic, especially the thicknesses of the layers crossed by X-rays at data collection (materials,

chamber height, etc). These parameters are now buried into the manuscript or missing, although they are essential in the choice of a delivery method for macromolecular crystallography.

A side view schematic of the dialysis chip including the thickness of each fabrication material (PMMA, NOA81 resin, Kapton tape and RC dialysis membrane) and the heights of the fluidic channel (45 µm) and the protein chamber (45 µm) is included in Figure 1 (Figure 1L). As we already explained while answering to the first comment of the reviewer, we acknowledge that the calculation of the total thickness of the chip (410 µm) that is exposed to the X-rays during *in situ* data collection was not thoroughly described in the manuscript. The thickness of the PMMA is 2 x 175 µm (PMMA is used as a substrate for the chip and a small piece is used for the closure of the protein chamber), of the Kapton tape 20 µm and the RC dialysis membrane is approximately 40 µm thick. These details are now illustrated in Figure 1L. Moreover, a color-based explanation has been added to all the steps of Figure 1 in order to guide the reader and facilitate the comprehension of the fabrication protocol.

In order to make these important details more evident in the protocol, we have changed Figure 1 and we have made the respective changes in the manuscript.

Manuscript lines 546 – 548:

Figure 1L illustrates a side view schematic of the dialysis chip where all the layers of the device and their respective thickness are indicated.

Manuscript lines 645 – 646:

(L) Side view schematic of the dialysis chip where all the layers of the device and their respective thickness are indicated.

ll.536, 634 and video 09:35 I think it is a bit bold to say that the high resolution data is not impacted, as this will mainly depend on the size and diffraction power of the crystals, compared to the device thickness. The investigated large and well-diffracting lysozyme crystals certainly yield high resolution in this case, but this says nothing of smaller crystals.

We would like to thank the reviewer for this relevant comment. In this protocol we describe the *in situ* X-ray diffraction data collection and treatment of lysozyme crystals grown on-chip with the microdialysis method. In this case, indeed, the large and well-diffracting lysozyme crystals yielded high-resolution data that could be processed accordingly and the electron density maps of the refined structures were obtained at less than 2 Å resolution. For the experiments performed with lysozyme, the background noise of the microchips didn't affect the treatment of the diffraction data sets. However, we acknowledge that this conclusion is not generic because, as the reviewer emphasizes it, the resolution of the diffraction data depends greatly on the size and the diffraction power of the protein crystals compared to the background noise generated by the microfluidic device. In a previous work (reference 19), we used the dialysis chip in order to collect *in situ* X-ray diffraction data from two other model proteins (Insulin from porcine pancreas and IspE from *Agrobacterium tumefaciens*). Partial diffraction data sets were collected from multiple crystals of both proteins and were merged to generate electron density maps at 2.1 Å and 2.3 Å resolution for insulin and IspE, respectively. The above mentioned case studies demonstrate the compatibility of the dialysis chip with *in situ* diffraction experiments at room temperature where detailed structural information can be revealed by collecting diffraction data from a large, well-diffracting crystal (lysozyme) or from significantly smaller, multiple crystals (insulin, IspE). However, we acknowledge that more challenging protein targets, producing crystals that might be even smaller, exhibiting less

diffraction power or being more susceptible to radiation damage, should be tested with our microchips. Therefore, in order to avoid any implication of a generic conclusion about high-resolution data, we suggest the following modifications:

Manuscript lines 588 – 589:

…that does not affect the treatment of high-resolution diffraction data of the large lysozyme crystals.

Manuscript lines 694 – 695:

…that does not affect the treatment of high-resolution diffraction data of the large lysozyme crystals.

Video 09:35: The audio part has been modified accordingly.

Another possible point of discussion: How about introducing reagents at the data collection stage to trigger time-resolved experiments?

Performing on-chip and *in situ* time-resolved studies is a possibility that we have considered and we assume that it would be interesting for the crystallographic community. We can imagine experiments where the crystals would grow on the dialysis chip and then the device would be set up on the appropriate beamline for *in situ* data collection. Reagents that could trigger time-resolved studies could be introduced within the microfluidic channel either manually (with the aid of a syringe) or automatically (with a pressure-driven fluidic system or a syringe-pump). However, there are some concerns that should be addressed in order to ensure the feasibility of time-resolved experiments. First of all, a major practical challenge is setting the chips on a beamline. So far, we have fabricated a support (Figure 3) for beamlines compatible with in plate diffraction experiments. Nevertheless, not all beamlines dedicated to macromolecular crystallography are compatible with in plate diffraction experiments. In this case, a support or a holder that could be easily adjusted on the head of a goniometer (like the holder used by Feiler *et al.* (reference 56) or Baxter *et al.* (reference 55)) should be designed and the chips could be mounted in many standard goniometer-based beamlines. Moreover, the diffusion of the reagents through the dialysis membrane has to be ensured in advance by selecting a membrane with the appropriate molecular weight cut-off (MWCO). The MWCO must be chosen accordingly to retain the protein sample and facilitate the diffusion of the crystallization precipitants and the reagents for time-resolved studies across the membrane. Apart from the diffusivity of the reagents across the dialysis membrane, preliminary experiments should be conducted in order to study diffusion times. The timescale in time-resolved experiments and the response time of the protein target to external triggers are crucial parameters. Therefore, it is also important to ensure that the diffusion time of the reagents through the dialysis membrane lies within the timescale of the diffraction experiment. Once these practical concerns are answered, we believe that the dialysis chip could be used for time-resolved experiments. In response to the reviewer's comment, we have added the following paragraph to the discussion section:

Manuscript lines: 732 – 737:

Finally, performing on-chip and *in situ* time-resolved studies is a future possibility that could be of significant interest to the crystallographic community. Therefore, by growing crystals on the dialysis chip and introducing the reagents into the microfluidic channel, either manually (using a syringe) or automatically (with a pressure-control fluid system or a syringe-pump), future efforts will focus on proving that the microfluidic chips can be successfully used to trigger time-resolved experiments on synchrotron beamlines.

Minor Concerns:

video 03:25: It is difficult to see where the RC membrane is deposited

We agree with the reviewer that it is difficult to see the RC dialysis membrane when being deposited on the central pillar of the PDMS stamp because both materials are optically transparent and the bench in the clean room where this manipulation takes place doesn't create any optical contrast to better visualize the membrane. For this reason, we added a photo (video 03:45) where the two PDMS molds (supported on a glass slide) and the RC membrane "sandwiched" between the two molds are placed on a black support. In this photo, the piece of the membrane can be seen clearly, while an arrow and a description has been added to facilitate the visualization.

video 08:05. Is the device leaking? I assume the protein solution goes between the NOA and unsealed PMMA, this needs to be clarified for the reader. Does it happen always when the protein solution touches the cavity side? Is it a problem?

In this part of the video, we can see the protein reservoir during the growth of lysozyme crystals on the microchip. The protein sample seems to be moving away from the dedicated cavity of the device. This is not a problem that we encounter always during on-chip crystallization experiments, however, it can be observed mainly when a pressure-driven system within inappropriate pressure range is used for the circulation of the crystallization solution within the fluidic channel. For the experiment visualized in the video (video 08:05), the protein sample was pipetted manually within the protein reservoir (as described in the protocol step 5.1) and a pressure-driven system was used for the introduction and circulation of the crystallization solution within the fluidic channel under a constant injection pressure of 100 mbar. In this case, we have noticed that it was difficult to confine the protein sample within the dedicated cavity of the device. In order to avoid this problem relatively low-pressure values should be applied while circulating the crystallization solution. We suggest an injection pressure of 20 – 60 mbar for solutions with a viscosity close to water viscosity (reference 19). However, even in the case that the protein sample is moving away from the protein reservoir, it doesn't leak outside the limits of the silicon grease. As we describe in the protocol (step 5.2), a thin layer of high-vacuum silicone grease is applied all around the protein reservoir. This layer of the silicone grease acts as a barrier when a movement of the protein sample occurs.

In order to clarify this observation and to guide the reader in cases where the protein sample is not perfectly confined in the protein reservoir, we have added a note in the protocol:

Manuscript lines 420 – 425:

NOTE: It is sometimes difficult to confine the protein sample within the dedicated cavity of the device (protein reservoir) when a pressure-driven system is used for the introduction of the crystallization solution within the fluidic channel (step 6.4). To avoid the problem mentioned above, relatively low pressure values should be maintained while circulating the crystallization solution. An injection pressure of 20 – 60 mbar for aqueous solutions or 50 – 150 mbar for more viscous solutions (PEGs, glycerol) is suggested[19].

What is the fabrication failure rate? Do you test devices before use?

We test the chips before setting up crystallization experiments by circulating the crystallization solution within the fluidic channel in order to ensure that the alignment of the two layers during the

fabrication process (protocol step 3.4) was successful. Bad alignment can lead to blockage of the inlet and outlet ports of the device. Another possible reason for the failure of the chips can be the blockage of the fluidic channel. In this case the NOA resin fills the cavity of the channel and leads to blockage during polymerization. This problem is rare and it is mainly encountered when we use the same PDMS molds several times, therefore, we suggest reusing them approximately 5 times after washing them properly (protocol lines 318-319).

Approximately 30 chips can be fabricated within 6 – 8 h. After testing them, a failure rate of 30% can be estimated.

It is possible to open the device to harvest a particularly nice crystal?

The protein reservoir could be opened by carefully removing the Kapton tape and the small piece of PMMA used to encapsulate the protein sample (protocol steps 5.3 – 5.4). We haven't performed such manipulation yet, as we have been mainly interested in the compatibility of the chips for *in situ* room temperature X-ray diffraction experiments. However, we can assume that carefully opening the protein reservoir could be accomplished in order to harvest crystals from within.

One could insist by writing already in the beginning or abstract that the functional element, RC membranes, are "off-the-shelf" or commercial, as this is one of the strong points of the paper.

We thank the reviewer for this suggestion that can highlight one of the main features of the dialysis chip. We have mentioned in several parts of the manuscript that the RC membranes used in this protocol are commercially available in various molecular weight cut-offs (MWCO). We added this information in the abstract too:

Manuscript lines 43 – 45:

The main feature of this microfabrication procedure lies on the integration of a commercially available, semipermeable regenerated cellulose dialysis membrane in between two layers of the chip.

For labs without easy access to clean room: maybe specify which steps absolutely need to be performed in a clean room.

Photolithography (steps 1.3.1 – 1.3.7) has to be performed in a clean room. The other steps of the protocol can be performed in any laboratory as long as some criteria are met:

1. A laminar flow hood is used to ensure a low level of particles in the air.
2. Yellow light in the room is used when working with the NOA81 resin (steps 3.6 – 3.11).
3. A source of UV light is available for the polymerization of the NOA81 resin (steps 3.7 and 3.11).

In order to make these points clear in the manuscript, we have made the following changes:

Manuscript lines 263 – 268:

NOTE: Steps 1.3.1 – 1.3.7 are performed in a clean room. The following steps of the protocol can be performed in any laboratory as long as a laminar flow hood is used, yellow light in the room is used

when working with the NOA 81 resin (steps 3.6 – 3.11) and a source of UV light is available for polymerizing the NOA 81 resin (steps 3.7 and 3.11).

l.68 aims to facilitate should be aims at facilitating

l.121: research instead of researches

We thank the reviewer for these comments which allow us to improve the manuscript.

Manuscript line 68: aims at facilitating

Manuscript line 144: research

You could cite Feiler et al, JoVE 2019 doi: 10.3791/59722 for a more complete review of state-of-the-art.

We thank the reviewer for this relevant reference. We have updated the manuscript accordingly:

Manuscript lines 133 – 143:

More recently, Feiler *et al.*[56] developed a sample holder for macromolecular *in situ* X-ray crystallography at cryogenic and ambient temperature with minimal background noise contribution. Specifically, the holder comprises of a plastic support, a transparent COC foil and a microporous structured polyimide foil. It was designed to replace the commonly used cover slides for setting up crystallization drops, while it allows in-place manipulation such as ligand soaking, complex formation and cryogenic protection without opening the crystallization drop or manually handling the crystals. Moreover, the sample holder can be removed from the crystallization plate and placed onto a magnetic base for *in situ* data collection at standard goniometer-based beamlines. For ambient temperature data collection, the COC foil is removed prior to the experiment and only the 21 µm-thick polyimide foil contributes to background scattering, which in this case is minimal.

l.346: pressure controlled: would a flow controlled system not work? For instance a syringe pump.

We are using a pressure-driven system in our laboratory for mixing and circulating the crystallization solution under a constant pressure value, or we manually introduce the solution within the fluidic channel with disposable syringes. However, we have performed on-chip crystallization experiments in other labs where syringe pumps were available and we can definitely propose that flow controlled systems work with the same efficiency. We added this information in the protocol in order to provide more options for fluid handling equipment:

Manuscript lines 382 – 384:

Commercially available kits are recommended for easy and precise control over the flow rate and are usually combined with automated pressure-driven or flow controlled (syringe pumps) systems for mixing and fluid handling.

Manuscript lines 455 – 456:

Inject the solution into the inlet point of the chip with a syringe or an automated pressure-driven fluidic system or a syringe pump, as described in steps 4.1 – 4.5.

Manuscript lines 460 – 461:

For the latter case, the use of an external pressure-driven system or syringe pump is recommended.

Manuscript lines 532 – 535:

The crystallization experiments are set up by manually pipetting the protein sample directly into the protein reservoir and introducing the crystallization solution into the linear fluidic channel with an automated pressure-driven system or syringe pump or manually with the aid of a syringe.

step 1.1: are the geometries used here to be found somewhere?

We have not published the CIF files with the geometries of the microfluidic devices. The chips and the fabrication protocol have been filed for a patent (reference 45).

l.389. Is washing required to reuse the chips, and how is this done?

The chips can be washed and reused several times as long as the RC dialysis membrane is still functional and the adhesion of the NOA resin on the PMMA substrate is not damaged. If these parts of the chip are damaged, leaks are observed verifying that the device can no longer be used. Washing the chips depends on the crystallization solution. In the case of low viscosity solutions (salts, buffers), the fluidic channel can be washed by merely introducing distilled water and let it flow for a few minutes. We have measured that 400 µL is the volume required in order to completely exchange a solution within the channel with another solution. So, a volume of water > 400 µL is sufficient to wash the fluidic channel from the crystallization solution. In the case of more viscous solutions (PEG, glycerol), we do not recommend reusing the chips since washing the channel just with water is not sufficient. The upper part of the chip, where the protein reservoir is located, can also be washed with distilled water and dried with pressurized air.

We have updated the protocol including these remarks:

Manuscript lines 432 – 441:

NOTE: The chips can be reused several times as long as the dialysis membrane and the adhesion of NOA on the PMMA substrate are not deteriorated. If these parts of the chip are damaged, leaks are observed verifying that the device can no longer be used. Washing the chips depends on the crystallization solution. In the case of low viscosity solutions (salts, buffers), the fluidic channel can be washed by merely introducing distilled water and let it flow for a few minutes. 400 µL is the volume required in order to completely exchange a solution within the channel with another solution. In the case of more viscous solutions (PEGs, glycerol), reusing the chips is not recommended since washing the channel only with water is not sufficient. The upper part of the chip, where the protein reservoir is located, can also be washed with distilled water and dried with pressurized air.

figure 1 K "dialysis chip." is not clear. The assembly of the 2nd PMMA and kapton layers are missing in the schematic.

A side view schematic of the dialysis chip including the second PMMA layer and the Kapton tape (missing in Figure 1K) has been included in Figure 1L.

step 2.3: is "to a height of approximately 5 mm." also valid for the second master?

Yes, the height of the pre-mixed PDMS poured into both SU-8 masters is approximately 5 mm. We have re-written the step 2.3 in the protocol in order to make this point clear to the reader:

Manuscript lines 279 – 281:

Pour the remaining 25 g of the PDMS into the second SU-8 master patterning only the pillars up to a height of approximately 5 mm (Figure 1C).

How long did it take to grow the lysozyme crystals?

We have tested several crystallization conditions with lysozyme (different precipitants and concentrations) and various concentrations of the protein sample and we have observed crystal growth even within 1 minute or after several hours from the onset of the experiment. The lysozyme crystals shown in Figure 3A grew within 1 h and the crystals in Figure 3B grew within 30 min.

Manuscript lines 609 – 610:

The lysozyme crystals shown in Figure 3A grew within 1 h and the crystals in Figure 3B grew within 30 min from the onset of the experiment.

What was the molecular weight cut-off used for lysozyme?

The molecular weight of lysozyme is 14.4 kDa and the molecular weight cut-off of the dialysis membrane used for these experiments was 6-8 kDa.

Manuscript lines 608 – 609:

… the MWCO of the RC dialysis membrane embedded within the microchips lies in the range of 6 - 8 kDa.

step 7.2.1: Add "For instance" at the beginning of the second sentence?

We thank the reviewer for this observation. Indeed, this is only an example of how diffraction data can be collected and the parameters depend on the beamline used for the experiments. In this section, we describe how we performed the *in situ* data collection at BM30A-FIP (ESRF).

Manuscript line 498: For instance, …

l.496: 45 um height sounds not consistent with the 50 um previously cited l. 199 and l. 278

We acknowledge that there is a misunderstanding concerning the height of the geometries that are first generated on the SU-8 masters with photolithography and then on the PDMS molds with soft lithography and we would like to explain this difference. During photolithography, the aim was to obtain the geometries of the device on the SU-8 masters with a height of 50 µm. However, once the two SU-8 masters were fabricated, we measured the height of these geometries (the height of the linear channel and the height of the pillars) with a profilometer. The measured value was approximately 45 µm. Therefore, the geometries on the PDMS molds and height of the channel and

the protein reservoir of the device is 45 µm (as shown in Figure 1L). We would like to thank the reviewer for this observation. Indeed, in line 278, the value should be 45 µm. We have made the following modifications in the manuscript:

Manuscript lines 222 – 223: For 50 µm nominal thickness, …

Manuscript lines 257 – 262:

NOTE: During photolithography, the aim is to obtain the geometries of the device on the SU-8 masters with a height of 50 µm. However, once the two SU-8 masters are fabricated, measure the height of the geometries engraved on the masters with a profilometer in order to acquire the experimental value. The measured value for both SU-8 masters fabricated for this protocol is approximately 45 µm.

Manuscript line 299: … exceeds vertically by 45 µm …

Manuscript line 315: … exceeds vertically by 45 µm …

l.522: Please detail the calculation leading to 410 um total thickness.

We explained the calculation of the total thickness in our response to the first comment of the reviewer. However, we can briefly describe again the calculation. The thickness of the PMMA is 2 x 175 µm (PMMA is used as a substrate for the chip and a small piece is used for the closure of the protein chamber), of the Kapton tape 20 µm and the RC dialysis membrane is approximately 40 µm thick. The total thickness of these materials is 410 µm.

Manuscript lines 574 – 575:

The thickness of the PMMA is 2 x 175 µm, of the Kapton tape 20 µm and the RC dialysis membrane is approximately 40 µm thick (Figure 1L).

ll. 487 and 649. It is not clear what is the protein solution consumption, is it 0.1/0.3 ul or 0.2/0.7 ul?

We have designed 4 prototypes for fabricating dialysis chips. The difference among these 4 designs is the volume of the protein reservoir. Originally, we could fabricate two different dialysis chips: one with a protein consumption volume of 0.2 µL and another of 0.7 µL. These results are presented in a previous publication (reference 19). Then, we designed two more prototypes with a protein consumption of 0.1 µL and 0.3 µL (presented in this protocol). The goal was to reduce the protein consumption per chip. For the experiments presented here, the lysozyme volume used per experiment (per chip) was 0.3 µL.

Manuscript lines 536 - 539:

Designs for fabricating chips with 0.1 µL or 0.3 µL maximum volume of the protein reservoir are shown in Figure 2A on the left and right respectively. Chips with a 0.2 µL or 0.7 µL maximum capacity for the protein sample are shown elsewhere[19].

Manuscript lines 607:

The volume of the protein sample in both experiments was about 0.3 µL

Manuscript lines 709 – 710:

For the prototypes presented in this work, the protein consumption per chip is limited down to 0.1 or 0.3 µL.

Reviewer #2

Manuscript Summary:

In this manuscript, authors have developed a device that allows users to not only screen protein crystallization conditions via microdialysis but also perform in situ X-ray diffraction analysis. This will allow rapid access to diffraction data, whilst minimizing the amount of sample consumed in crystallization screening and the time required for harvesting and mounting the crystals, which is meaningful for protein structure determination. Furthermore, in this manuscript, the authors presented a detail protocol to illustrate how to fabricate and use this device for protein crystallization screening and in situ X-ray diffraction analysis. It is an interesting work. Thus, I recommend it is published in JOVE.

We would like to thank the reviewer for reading our manuscript and recommending it for publication in JoVE.

Reviewer #3

Manuscript Summary:

The revision is well written, and the method described here is clear and has been demonstrated well.

We would like to thank the reviewer for reading our manuscript. We are satisfied that the protocol is clearly described and comprehended.